

DTIC FILE COPY



AD-A212 439

DEPARTMENT OF DEFENCE
DEFENCE SCIENCE AND TECHNOLOGY ORGANISATION
AERONAUTICAL RESEARCH LABORATORY

MELBOURNE, VICTORIA

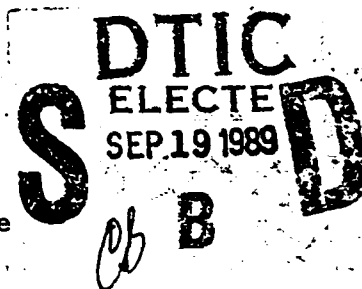
Aerodynamics Report 174

AXISYMMETRIC VORTEX BREAKDOWN PART II
PHYSICAL MECHANISMS

by

G.L. BROWN and J.M. LOPEZ

Approved for Public Release



This work is copyright. Apart from any fair dealing for the purpose of study, research, criticism or review, as permitted under the Copyright Act, no part may be reproduced by any process without written permission. Copyright is the responsibility of the Director Publishing and Marketing, AGPS. Inquiries should be directed to the Manager, AGPS Press, Australian Government Publishing Service, GPO Box 84, Canberra, ACT 2601.



Commonwealth of Australia
JANUARY 1988

89 9 18 051

THE UNITED STATES NATIONAL
TECHNICAL INFORMATION SERVICE
IS AUTHORIZED TO
REPRODUCE AND SELL THIS REPORT

DEPARTMENT OF DEFENCE
DEFENCE SCIENCE AND TECHNOLOGY ORGANISATION
AERONAUTICAL RESEARCH LABORATORY

Aerodynamics Report 174

**AXISYMMETRIC VORTEX BREAKDOWN PART II:
PHYSICAL MECHANISMS**

by

G.L. Brown
and
J.M. Lopez

SUMMARY

In Part I of this study (Lopez, 1988), numerical solutions of the axisymmetric Navier-Stokes equations are presented and compared with results from experiments for a confined cylindrical flow. The details of the vortex breakdown phenomenon are calculated with a high degree of accuracy. From solutions over a range of parameters the essential features of the flow are obtained. These solutions also provide flow quantities such as the vorticity and the pressure throughout the volume which would be difficult to obtain from experiments. In this paper the solutions are explored and the essential physical mechanisms of vortex breakdown in this particular geometry are identified. These mechanisms, which rely on the production of a negative azimuthal component of vorticity as a result of the stretching and tilting of the predominantly axially directed vorticity vector, are elucidated with the aid of a simple, steady, inviscid, axisymmetric equation of motion. This equation has been a starting point for most studies of vortex breakdown but a departure in the present study is that it is explored directly and not through perturbations of an initial stream function. The findings are then generalised to the case of vortex breakdown in swirling pipe flows.



(C) COMMONWEALTH OF AUSTRALIA 1988

POSTAL ADDRESS: Director, Aeronautical Research Laboratory,
P.O. Box 4331, Melbourne, Victoria, 3001, Australia

CONTENTS

	Page No.
1. INTRODUCTION	1
2. CONFINED SWIRLING FLOWS	2
2.1 Summary of the principal features of the flow	2
2.2 Theoretical considerations	2
2.3 Physical mechanisms	6
3. SWIRLING FLOWS IN PIPES AND IN A FREE STREAM	11
3.1 Preliminary considerations	11
3.2 Physical mechanisms	13
3.3 Comparison with experiment	14
4. CONCLUDING REMARKS	16

References

Appendix 1

Figures

Distribution

Document Control Data



Accession For	
NTIS GRA&I	<input checked="" type="checkbox"/>
DTIC TAB	<input type="checkbox"/>
Unannounced	<input type="checkbox"/>
Justification	
By	
Distribution/	
Availability Codes	
Dist	Avail and/or Special
A-1	

1. Introduction

The attraction of the confined swirling flow of Part I to a study of vortex breakdown is that the flow is defined by only four variables, H , R , Ω and ν , each of which, in an experiment, can be very accurately determined. Similarly, from a numerical point of view, the flow is confined in a fixed volume with very well defined boundary conditions. It was hoped that if numerical solutions for various H/R and $Re = \Omega R^2/\nu$ could be obtained which very accurately predicted the resulting flow in such a well defined experiment then the physical mechanisms of vortex breakdown could be elucidated from these solutions and further, that these mechanisms might be generalised to the swirling flows of more practical significance in pipes and in a free stream.

Many features of vortex breakdown have been well recognised and the early works of Squire (1960) and Benjamin (1962) have been the starting point for many subsequent studies. A departure in the present study from these formulations is that the numerical solutions are explored not from a consideration of perturbations to an initial stream function but more directly from the development of the azimuthal component of vorticity. This leads to criteria which depend essentially on the relationship between the angle of the vorticity vector and the velocity vector on stream surfaces upstream of breakdown.

The numerical results in Part I demonstrate the accuracy with which the experimental results can be predicted for confined flows in which 'vortex breakdown' develops and this paper, Part II, explores the underlying physical mechanisms which account for the essential features of the flow and are important in 'vortex breakdown'.

2. Confined swirling flows

2.1 Summary of the principal features of the flow.

As suggested in Part I, for the confined flow in which $H/R = 2.5$ and $Re > 1600$, the central core flow, i.e. the flow returning towards the rotating endwall, might be regarded as practically inviscid apart from the recirculation zone and the fluid that passes near to it. This first approximation, expected to be increasingly valid as Reynolds number increases, is supported by Figure 1 which shows contours of the streamfunction ψ , the angular momentum, or circulation, Γ and the total head H . A detailed comparison between these contours shows that in this central core region Γ and H are approximately constant on stream surfaces, apart from those surfaces within and near to the recirculation bubble where Γ and H are relatively small. An approximation that they are constant on the stream surface would seem unlikely to change the *principal* features of the flow. Of course, the experiments and the numerical calculations show that this core flow is critically dependent on Reynolds number but mainly in the sense, it seems, that Re determines an 'upstream' distribution of $\Gamma(r)$ and $H(r)$ and that once this distribution is established the subsequent core flow, in which vortex breakdown occurs, is largely an inviscid rotational flow apart from the flow within and near to the recirculation zones.

The most striking features of this core flow are the divergence from an upstream narrow core to a much larger diameter flow which is almost in solid body rotation, and correspondingly, the development of a wave as a result of an 'overshoot' in the initial divergence. The apparent effect of increasing Reynolds number is to change the upstream distribution of $\Gamma(r)$ and $H(r)$ in a way such as to increase the initial divergence, increase the 'overshoot', reduce the wavelength of the resulting wave and reduce the 'damping' of this wave. The contours of the streamfunction (Figure 2 from Part I) suggest that the appearance of recirculation bubbles is related to the waviness in the outer flow. These preliminary observations provide useful approximations and working hypotheses which are explored in the remainder of Section 2.

2.2 Theoretical considerations.

Steady, inviscid, axisymmetric swirling flow is particularly interesting in that it can be looked at from the point of view of an interaction between the total head and the angular momentum of the fluid (both of which are conserved on a stream surface), or, in terms of a balance between the radial pressure gradient and the centrifugal force, or, in terms of the generation of the azimuthal component of vorticity through the stretching

and tilting of vortex lines.

The relationship between these three different perspectives is as follows. In terms of the radial pressure gradient and the centrifugal force, the other radial acceleration terms are

$$u \frac{\partial u}{\partial r} + w \frac{\partial u}{\partial z} = \frac{v^2}{r} - \frac{1}{\rho} \frac{\partial p}{\partial r}. \quad (1)$$

In terms of the angular momentum (or circulation) $\Gamma = rv$, and the total head $H = p/\rho + (u^2 + v^2 + w^2)/2$, (1) may be written as

$$w \frac{\partial u}{\partial z} = \frac{\Gamma}{r^2} \frac{\partial \Gamma}{\partial r} - \frac{\partial H}{\partial r} + u \frac{\partial u}{\partial r}. \quad (2)$$

Thirdly, since the azimuthal component of vorticity is $\eta = \partial u / \partial z - \partial w / \partial r$, then from (2)

$$w\eta = \frac{\Gamma}{r^2} \frac{\partial \Gamma}{\partial r} - \frac{\partial H}{\partial r}, \quad (3)$$

or, since the streamfunction ψ is determined by $u = -1/r \partial \psi / \partial z$ and $w = 1/r \partial \psi / \partial r$ and since Γ and H are constant on ψ , it follows from (3) that

$$\eta = \frac{\Gamma}{r} \frac{d\Gamma}{d\psi} - r \frac{dH}{d\psi}. \quad (4)$$

Equation (4) has been a starting point for most discussions of vortex breakdown. Following Squire (1960), it is usually rewritten by replacing η with $-1/r \nabla^2 \psi$. Notwithstanding that Γ and H are functions of r and z , the equation as it stands is of such a simple form that we have pursued its implications more directly. In particular, if the curve C in the r, z plane whose radius r is given by $r = \sigma(z)$ is chosen such that on C the streamfunction is a constant, i.e. $\psi(r, z) = \psi_1$, then on C

$$\eta(z) = \frac{\Gamma(\psi_1)}{\sigma} \Gamma'(\psi_1) - \sigma H'(\psi_1), \quad (5)$$

$$d\psi = 0 \text{ and } u = w\sigma'(z); \quad (6)$$

or, on a stream surface

$$\eta(z) = \frac{A}{\sigma} - B\sigma, \quad (7)$$

and

$$d\eta = -\left(\frac{A}{\sigma^2} + B\right)d\sigma, \quad (8)$$

where $A = \Gamma(\psi_1)\Gamma'(\psi_1)$ and $B = H'(\psi_1)$.

Equation (7) is remarkable since it provides such a simple expression for one component of the vorticity in terms only of the radius of the stream surface yet in a complex flow where the vorticity is three dimensional, not normal to the velocity, and where the stretching of vorticity is an essential mechanism in the flow.

Further insight into the implications of equations (7) and (8) is gained if it is assumed that at some upstream station z_0 and on a particular stream surface $\psi = \psi_1$, the radius of the stream surface is σ_0 and the azimuthal and axial components of both the velocity, i.e. v and w , and vorticity, i.e. η and ζ , are known and have the values v_0 , w_0 , η_0 and ζ_0 (see Figure 2). In this case A and B may be determined simply, since

$$r\zeta = \frac{\partial \Gamma}{\partial r} = rw \frac{d\Gamma}{d\psi},$$

so that on ψ_1

$$\Gamma'(\psi_1) = \frac{\zeta_0}{w_0},$$

and

$$A = \Gamma(\psi_1)\Gamma'(\psi_1) = \frac{\sigma_0 v_0}{w_0} \zeta_0.$$

B may be determined from (7) evaluated at $z = z_0$. If $\eta_0 \neq 0$, then

$$B = \frac{\eta_0}{\sigma_0} \left(\frac{v_0 \zeta_0}{w_0 \eta_0} - 1 \right),$$

and if $\eta_0 = 0$ then

$$B = \frac{v_0 \zeta_0}{\sigma_0 w_0}.$$

Thus from (7) the equation for η on the stream surface downstream from z_0 is

$$\eta = \alpha_0 \zeta_0 \left(\frac{\sigma_0}{\sigma} - \frac{\sigma}{\sigma_0} \right),$$

for $\eta_0 = 0$, or

$$\frac{\eta}{\eta_0} = \frac{\sigma_0}{\sigma} \left(\frac{\alpha_0}{\beta_0} \right) - \frac{\sigma}{\sigma_0} \left(\frac{\alpha_0}{\beta_0} - 1 \right), \quad (9)$$

for $\eta_0 \neq 0$, where $\alpha_0 = v_0/w_0$ and $\beta_0 = \eta_0/\zeta_0$ are the tangents of the helix angle for the velocity and vorticity respectively. Thus, downstream of z_0 , the ratio of η on a stream surface to its value on the surface at z_0 , depends only on the ratio of the tangents of the helix angles of the vorticity and velocity on the surface at z_0 and on the ratio of the radius of the stream surface to the radius at z_0 .

Equation (9) has interesting implications. Assuming that inviscid behaviour is the dominant mechanism responsible for the rapid divergence of the streamtubes observed

in vortex breakdown, a reasonable hypothesis (in the absence of bodies in the flow field) is that the development of a negative azimuthal component of vorticity on some stream surfaces is necessary if the axial velocity is to be brought to zero (see Figure 2.)*

If this is so then from equation (9) it is clear that, for η_0 positive, η will only become negative on a diverging stream surface if $\alpha_0 > \beta_0$, i.e. $v_0/w_0 > \eta_0/\zeta_0$. A helix angle for the velocity which exceeds that of the vorticity on some stream surfaces would seem therefore to be a necessary condition for vortex breakdown to occur since, from (9), as σ/σ_0 increases from unity, then for $\alpha_0 > \beta_0$, η/η_0 decreases to zero and becomes negative at a sufficiently large σ/σ_0 . Figure 3 illustrates the behaviour and the dependence on α_0/β_0 .

The development of negative η on stream surfaces will induce a negative axial velocity on the axis which, by continuity, will lead to a further increase in σ and correspondingly, a further increase in negative vorticity, etc. This can be seen as a kind of 'positive feedback' which accounts for the relatively rapid divergence of stream surfaces in the proximity of 'breakdown'. In essence, however, this is a matter of compatibility between the velocity (U) and the vorticity ($\nabla \times U$) arrived at from a consideration of the dynamics of vorticity and continuity. It follows that a necessary condition for subsequent vortex breakdown (in the absence of viscous or turbulent diffusion and the absence of bodies in the flow field) would seem to be that $v_0/w_0 > \eta_0/\zeta_0$.

A reduction in azimuthal vorticity with increasing radius is readily understood physically for the simple case of a flow which is cylindrical upstream and has $\eta = 0$. If two material points on a vortex line (which is axial in this cylindrical flow) move with the fluid and the leading point advances to a location where the radius has begun to increase, then this leading point will experience a reduction in azimuthal velocity due to the conservation of Γ on the stream surface. The material line between the points is therefore stretched and tilted, and since the vorticity moves with this material line, a negative azimuthal component of vorticity is generated. This accords of course with the

* For simplicity, in this paper z is taken to increase in the direction of the primary axial velocity in the core flow and correspondingly negative azimuthal vorticity will induce an axial velocity in the opposite direction. In Part I increasing z is in the opposite direction away from the rotating end wall and the sign of the corresponding azimuthal vorticity is the reverse of its sign in this paper.

$\eta_0 = 0$ case of equation (9). More generally however, for $\eta_0 \neq 0$, then from (8) or (9),

$$\frac{d\eta}{d\sigma} = \frac{-\eta_0}{\sigma_0} \left(\left(\frac{\sigma_0^2}{\sigma^2} + 1 \right) \frac{\alpha_0}{\beta_0} - 1 \right),$$

which implies not a reduction but an increase in azimuthal vorticity with increasing radius, i.e. in the absence of a body in the flow field, 'negative feedback' in terms of the above compatibility argument, if

$$\left(\frac{\sigma_0^2}{\sigma^2} + 1 \right) \frac{\alpha_0}{\beta_0} < 1.$$

It follows that for $\sigma/\sigma_0 \geq 1$ and η_0 positive then for $\alpha_0/\beta_0 < 0.5$, $d\eta/d\sigma > 0$; for $0.5 < \alpha_0/\beta_0 < 1$, η remains positive and at sufficiently large σ/σ_0 , $d\eta/d\sigma > 0$; and only for $\alpha_0/\beta_0 > 1$, does η become negative for sufficiently large σ/σ_0 . (See fig. 3). [This more general result is not easily interpreted physically but from an extension of the above simple argument for the case of $\eta = 0$, one can see that if $\beta_0 \gg \alpha_0$ it is plausible that the vorticity vector could be rotated to an even larger helix angle by a change in the velocity vector with radius (v and w decrease with increasing r) so that the result that $d\eta/d\sigma > 0$ for $\beta_0 > 2\alpha_0$ is not as surprising as it may seem at first sight.]

An analogy in these terms with supersonic flows seems possible in the sense that strong negative feedback ($d\eta/d\sigma$ positive) suggests stability and an absence of waves on the stream surface. There is not a simple connection, however, between this result and the supercritical, subcritical distinction described by Benjamin (1962, 1967).

With these general considerations in mind, the vortex breakdown features of the confined swirling flow may be interpreted as follows.

2.3 Physical mechanisms.

The summary in Section 2.1 and these theoretical considerations suggest that an important question to ask is why the strong vortical core flow begins to diverge? A simple, if simplistic answer is clear from equation (1). Downstream from the point where $u = 0$ and the stream surface has its smallest radius (or, more generally, downstream from a region in which the flow is cylindrical) there will be divergence, i.e. positive $\partial u/\partial z$ only if the centrifugal force exceeds the radial pressure gradient [in the absence of viscous stresses]. For the confined flow, this imbalance clearly arises from the fact that the radial distribution of Γ and H in the narrow upstream core region is determined by the 'upstream' history of a fluid particle as it travels on its closed stream surface. In

particular, the particle acquires and loses most of its angular momentum and total head through the action of viscous stresses in the boundary layers near the surfaces of the volume (Figure 1). There is no reason why the radial distributions of Γ and H should lead to $\eta = 0$ (equation (3)), or to cyclostrophic balance (equation (1)). Quite the contrary, in fact, since the turning of the flow from radially inward towards the lower rotating endwall requires the centrifugal force to exceed the radial pressure gradient. This is supported by Figure 4 which shows the calculated contours of $v^2/r - 1/\rho \partial p / \partial r$ for the case $Re = 1994$, $H/R = 2.5$. [These contours provide an interesting view of the force field; they are not surprising in the sense that they accord with the waviness of the stream surface and the corresponding sinusoidal like variation in the radial acceleration.]

The reason for the initial 'overshoot' in the divergence of the stream surfaces and the subsequent waviness can be seen as follows. From (4), we have

$$\frac{\partial u}{\partial z} = \frac{\Gamma}{r} \frac{d\Gamma}{d\psi} - r \frac{dH}{d\psi} + \frac{\partial w}{\partial r}. \quad (10)$$

For the confined swirling flow, if $z = z_0$ where $u = 0$ and $\partial u / \partial z$ has a local maximum, i.e. where a stream surface has its smallest radius, then on a particular stream surface of radius $r = \sigma(z)$, whose radius is $\sigma = \sigma_0$ at $z = z_0$,

$$\left. \frac{\partial u}{\partial z} \right|_{\sigma} - \left. \frac{\partial u}{\partial z} \right|_{\sigma_n} = A \left(\frac{1}{\sigma} - \frac{1}{\sigma_0} \right) - B(\sigma - \sigma_0) + \left. \frac{\partial w}{\partial r} \right|_{\sigma} - \left. \frac{\partial w}{\partial r} \right|_{\sigma_n}, \quad (11)$$

where A and B are the particular values of $\Gamma d\Gamma/d\psi$ and $dH/d\psi$ on this stream surface.

The characteristic shape of the stream surface downstream from z_0 can be explored as follows. Since u is $w\sigma'$ (equation (6)), equation (11) may be approximated by

$$w(\sigma)\sigma'' - w(\sigma_0)\sigma''(z_0) \simeq A \left(\frac{1}{\sigma} - \frac{1}{\sigma_0} \right) - B(\sigma - \sigma_0) + \left. \frac{\partial w}{\partial r} \right|_{\sigma} - \left. \frac{\partial w}{\partial r} \right|_{\sigma_n}. \quad (12)$$

(Note that $w(\sigma) = w(\sigma_0)$ corresponds with a small perturbation linearization). Immediately downstream of z_0 for example, the diverging stream surface implies an increasing σ and σ'' is expected to decrease, i.e. $\sigma''(z) < \sigma''(z_0)$ because $A(1/\sigma - 1/\sigma_0)$ and $-B(\sigma - \sigma_0)$ are both negative, assuming, in accord with Section 2.2, that since breakdown occurs, $\alpha_0 > \beta_0$ and B is, therefore, positive. Note however that $\partial w / \partial r|_{\sigma} - \partial w / \partial r|_{\sigma_n}$ is expected to be positive because diverging stream surfaces imply by continuity, a reduction in w and a relatively larger reduction in w is expected near $r = 0$ than at large r , ($\partial w / \partial r|_{\sigma_n}$ is expected to be negative). Thus, downstream of z_0 , σ'' is expected to decrease, but the rate at which this occurs will depend on w . The continued divergence of the flow and

corresponding reduction in σ'' therefore leads to a radius of the stream surface at which $\sigma'' = 0$ (infinite radius of curvature of the stream surface). At this point the local slope σ' , is a maximum. Since the flow continues to diverge downstream from this point, σ'' becomes negative and the stream surface begins to reduce in slope, turning back towards the axis.

An alternative explanation for the flow divergence and subsequent turning of the flow towards the axis may be sought in terms of equation (1). An imbalance in $v^2/r - 1/\rho \partial p / \partial r$ gives rise to a positive value of σ'' . On this diverging stream surface, v^2/r is decreased due to the conservation of Γ and at the same time, w and v are reduced due to the divergence, leading to an increased pressure with relatively larger changes for small r and a reduction in the radial pressure gradient. While not self-evident, the reduction in v^2/r must exceed the reduction in $\partial p / \partial r$ since, as outlined above, σ'' approaches zero.

A further alternate and more direct explanation may be sought in terms of the kinematics of vorticity (equation (4)). As discussed in Section 2.2, for positive B , ($\alpha_0 > \beta_0$) the diverging flow gives rise to a reduction of the positive azimuthal component of vorticity and the development, with increasing radius, of negative azimuthal vorticity. In this case, the 'positive feedback' discussed, leads to the further development of negative azimuthal vorticity and the divergence is expected to continue until the negative azimuthal vorticity grows to a sufficiently large magnitude for it to turn the diverging flow back towards the axis.

The fact that the divergence 'overshoots' and that a wave in the stream surface results may be approximately seen by linearising equation (12) about the radius $\sigma = \sigma_1$ at which $\sigma'' = 0$. Thus for $\sigma = \sigma_1 + \xi(z)$, then from (12)

$$w_1 \xi'' \simeq - \left(\frac{A}{\sigma_1^2} + B \right) \xi, \quad (13)$$

where perturbations in $\partial w / \partial r$ have been neglected compared with $\partial u / \partial z$. A wave in the stream surface is therefore established with wave number k given by $w_1 k^2 \simeq A/\sigma_1^2 + B$.

The shape of a characteristic stream surface in the core flow downstream of z_0 can be summarized as follows. The stream surface $\sigma(z)$ diverges from σ_0 to σ_1 and σ'' is reduced from a maximum to zero. At the radius $\sigma = \sigma_1$, the positive slope σ' is a maximum and the flow continues to diverge, $\xi > 0$, but σ'' , or ξ'' , becomes negative and the surface begins to turn towards the axis. This overshoot of the radial displacement leads to a subsequent oscillation in the displacement of the stream surface about $\sigma = \sigma_1$.

i.e. $\xi = 0$. The wavelength of this displacement is approximately

$$\lambda \simeq 2\pi w_1^{0.5} \left(\frac{\Gamma}{\sigma_1^2} \frac{d\Gamma}{d\psi} + \frac{dH}{d\psi} \right)^{-0.5}, \quad (14)$$

where w_1 is the axial velocity at $r = \sigma_1$.

Using the expressions for A and B from Section 2.2, the wavelength can also be approximated by

$$\lambda/\sigma_1 \simeq 2\pi \left(\frac{w_1}{\eta_0 \sigma_0} \right)^{0.5} \left[\frac{\sigma_1^2}{\sigma_0^2} \left(\frac{\alpha_0}{\beta_0} - 1 \right) + \frac{\alpha_0}{\beta_0} \right]^{-0.5} \quad (15)$$

A comparison between the wavelength evaluated from (15) and that determined from the periodicity in the numerical solution is presented in Table 1. The wavelength predicted by equation (15) was evaluated on a stream surface where Γ and H are approximately constant (selected by comparing the contours of Γ , H and ψ as in Figure 1). The wavelength from the numerical solution was determined from the contours of $v^2/r - 1/\rho \partial p / \partial r$. Of course, the wavelength found in both cases can be regarded only as a typical wavelength. As expected the agreement (approximate) in Table 1 between the inviscid prediction of equation (15) (and equation (14)) and the numerical solution increases with increasing Reynolds number. The difference between the predictions of equations (14) and (15) reflects the fact that equation (14) is evaluated in the region of the waves, where the flow is most inviscid, whereas equation (15) assumes inviscid flow from z_0 where the radius of the stream surface is a minimum. Closer examination of Figure 1 shows that the approximation that Γ and H are constant on stream surfaces is not accurate in this region. Particularly at lower Reynolds numbers it is not surprising therefore that the azimuthal viscous stresses should lead to some additional reduction in the azimuthal component of vorticity in this region and correspondingly that equation (9) would predict a larger radius than the numerical solution, for a given reduction in η . This is consistent with the prediction from equation (15) of a shorter wavelength than is found from the numerical solution.

As a check whether the model describes the principal features of the flow, however, the agreement seems satisfactory. In accord with this discussion and that of Section 2.2 the subsequent development of a second recirculation zone could be expected if the wave is of sufficient amplitude for the subsequent diverging stream surface to develop sufficient negative azimuthal vorticity to again bring the axial velocity to zero. The

converging stream surface, by contrast, generates positive azimuthal vorticity which accelerates the axial flow.

The principal features and physical mechanisms of the 'breakdown' in the confined swirling flow are therefore comprehensible in terms of inviscid phenomena. The initial divergence from a narrow core is the result of the upstream radial distribution of H and Γ , the subsequent waviness of the stream surface is a result of a stationary inertial or centrifugal wave and the development of one or more recirculation zones is a consequence of the generation of negative azimuthal vorticity through the stretching and tilting of vortex lines in a diverging, swirling inviscid flow. At a Reynolds number above that at which breakdown first occurs, the apparent 'critical' dependence of the flow on Re , discussed in Part I, arises essentially from the dependence of the radial distributions of Γ and H (in the core flow) on the action of viscous stresses in the boundary layer regions near the walls. At higher Reynolds number the core flow behaves in a broadly inviscid manner and the recirculation zones appear to have relatively little dynamical significance, except insofar as they are within the region of strong negative azimuthal vorticity.

These mechanisms which appear to account for the principal features of breakdown in the confined flow led to our considering their applicability to swirling flows in pipes.

3. Swirling flows in pipes and in a free stream

3.1 Preliminary considerations.

The relatively sudden appearance of a rapid divergence in the stream surfaces, and the corresponding appearance of recirculation zones, occurs in some swirling pipe flows and in the vortex breakdown observed in flows over delta wings at high angle of attack. A comparison with the 'breakdown' observed in the confined swirling flow suggests that these breakdown regions are qualitatively similar, at least up to the first recirculation region. An essential difference however, is that for swirling pipe flows and to some extent the delta wing flow, the 'upstream' region may be regarded as essentially a cylindrical flow for which initially $v^2/r = 1/\rho \partial p / \partial r$ or, in terms of equation (4)

$$\frac{\partial u}{\partial z} = \frac{\Gamma}{r} \frac{d\Gamma}{d\psi} - r \frac{dH}{d\psi} + \frac{\partial w}{\partial r} = 0.$$

For this case, the question that is immediately posed is how does 'breakdown' begin? One of us (Lopez) has obtained time dependent numerical solutions of the Navier Stokes equations for various swirling flows in a pipe by the methods outlined in Part I. The particular family of flows that has been calculated is given at $t = 0$ by a zero radial component of velocity, an azimuthal component of velocity

$$v = \frac{av_c}{r(1 - e^{-1})} (1 - e^{-r^2/a^2}), \quad (16)$$

and an axial component of velocity

$$w = W_\infty (1 + W_c e^{-r^2/a^2}). \quad (17)$$

These distributions have been found to be good fits to various experimental observations of vortices undergoing breakdown (eg. Garg & Leibovich, 1979). This azimuthal velocity distribution has the further merit that it has the same form as the exact solution for the diffusion of vorticity from a line vortex (Burgers, 1940).

The distributions of velocity in equations (16) and (17) have the corresponding azimuthal and axial components of vorticity,

$$\eta = \frac{2W_\infty W_c r}{a^2} e^{-r^2/a^2},$$

and

$$\zeta = \frac{2v_c}{a(1 - e^{-1})} e^{-r^2/a^2},$$

and in terms of the helix angles for velocity and vorticity discussed in Section 2.2, on stream surfaces at $z = 0$

$$\frac{\alpha_0}{\beta_0} = \left(\frac{e}{e-1}\right)^2 \frac{V_c^2 a^2 (1 - e^{-r^2/a^2})}{W_c r^2 (1 + W_c e^{-r^2/a^2})},$$

where $V_c = v_c/W_\infty$. Within the range $1 < W_c < 2$, α/β does not vary substantially for stream surfaces for which $0 < r/a < 1$ and at $r/a = 1$

$$\frac{\alpha_0}{\beta_0} = \frac{W_c e^2}{(e-1)(W_c + e)} \frac{V_c^2}{W_c^2}.$$

This relationship between α_0 and β_0 at $r/a = 1$ for various values of V_c and W_c is shown in figure 5 and the regime is marked for which the inviscid criterion for vortex breakdown ($\alpha_0 > \beta_0$) is met. The points where numerical solutions have been obtained are also given in the figure. For a particular flow to be discussed, $V_c = 1.5$, $W_c = 1.25$ and at $r = a$, α_0/β_0 is 1.95.

The initial conditions for the calculated flows are that equations (16) and (17) are the velocities at $t = 0$ for all z . The upstream boundary condition is that these velocities are imposed for $t > 0$. The radial boundary condition at $r = R$ is $u = 0$, $\partial v/\partial r = 0$ and $\eta = 0$. The usual outflow condition, $\partial/\partial z = 0$ is applied. (A further discussion of these boundary conditions and their implementation is set out in Appendix I.) With these initial and boundary conditions the presence of viscosity is essential for the evolution of this flow - inviscid flow would not change with time. An example of the development of the flow for a particular Reynolds number is shown in Figure 6. Of course, at very low Reynolds number, viscous diffusion dominates the flow development. At higher Reynolds numbers however, we have found that for the same initial cylindrical velocity distributions, the time taken before a recirculation zone appears increases with Reynolds number (defined as $Re = W_\infty a/\nu$). Unlike the confined swirling flow, for these flows it is the diffusion of axial vorticity which leads initially to $v^2/r - 1/\rho \partial p/\partial r$ becoming positive. Alternatively, we anticipate that it must be the diffusion of vorticity which leads to a radial redistribution of Γ and to the stretching and tilting of vortex lines (due to the axial change in v), with a corresponding reduction in the initial positive azimuthal component of vorticity with axial distance, and the subsequent beginning of an 'inviscid' breakdown process.

This broad view of the likely role of viscosity and the development of azimuthal vorticity is illustrated in the calculations of v , η and ψ shown in Figure 6 and leads to the following more detailed considerations.

3.2 Physical Mechanisms.

In considering the results shown in Figure 6, particular attention is drawn to the reduction of the azimuthal velocity and vorticity with distance downstream. Initially, this reduction is due to viscous effects, but it is clear that by $t = 40$, there is a slight divergence of streamlines which, by the inviscid mechanisms of section 2, contributes to this reduction. At $t = 80$ this azimuthal vorticity has been reduced to zero on stream surfaces at a downstream distance of about $20a$ and out to a radius of about a and a further divergence of these stream surfaces has generated a negative azimuthal component. The positive feedback mechanisms described in section 2.2 drive this further development of a negative azimuthal component leading, by $t = 240$, to a small recirculation zone on the axis, rapid changes in the azimuthal vorticity ahead of this region where the streamlines diverge, and the evident propagation upstream of the region of negative azimuthal vorticity due to its own induced velocity. The subsequent appearance of a second recirculation zone located at a distance downstream where the outer stream lines diverge and where the azimuthal component of the vorticity has a second maximum is consistent with the establishment of a wave on the outer stream surfaces by essentially the same mechanism as in the confined swirling flows.

Further insight into the mechanics of the flow is obtained from a detailed comparison between the results shown in figures 7(b), 7(c), and 7(d). Figures 7(a) and 7(b) show the development of the flow for which $V_c = 1.75$, $W_c = 1.6$ and $Re = 300$ (with a corresponding $\alpha_0/\beta_0 = 1.91$) from $t = 227$ to $t = 250$. Figure 7(c) shows a corresponding development in an unphysical case in which, for the above flow, at $t = 227$ the viscosity is suddenly doubled, (i.e. Reynolds number reduced from 300 to 150). Figure 7(d) is the case in which the viscosity is suddenly halved ($Re = 600$) at $t = 227$. A comparison between figures 7(b) and 7(c) shows that the subsequent effect of a sudden increase in the viscosity is to diffuse the axial vorticity and increase the initial divergence of streamlines but reduce the magnitude of the maximum negative component of azimuthal vorticity from -1.84 to -1.37, to reduce the size of the recirculation bubble, and reduce the rate at which the field of negative vorticity (and the bubble) propagate upstream. By contrast, comparison between figures 7(b) and 7(d) shows that reducing viscosity reduces the diffusion of axial vorticity which reduces the initial divergence of streamlines; the presence of the bubble and divergence of the stream-lines immediately ahead of it and the reduced diffusion of axial vorticity increases the magnitude of the maximum negative

component of azimuthal vorticity that is reached from -1.84 to -2.17. The bubble is correspondingly larger, it propagates upstream a little more quickly, the amplitude of the wave on the outer stream surface is greater and a small second recirculation zone begins to emerge.

These results are quite consistent with the discussion in section 2.2. For this flow the necessary criterion for breakdown to occur ($\alpha_0 > \beta_0$) is satisfied. The development of the flow requires viscosity to initiate a reduction of the azimuthal components of vorticity and velocity with distance downstream and to initiate the divergence of the streamlines. However, the development of the breakdown is essentially an inviscid process driven by the positive feedback mechanisms described in section 2.2. The reduction in viscosity introduced after a bubble has appeared, figure 7(d), shows the dominant role that this inviscid mechanism plays. In some respects the phenomenon in this swirling pipe flow case is not unlike boundary layer transition in the general sense that the initial development (Tollmein-Schlichting waves in boundary layer transition) depends on viscosity and the final transition process is a consequence of 'positive feedback' in the generation, in that case, of a longitudinal component of vorticity.

3.3 Comparison with experiment.

While more detailed comparisons with experiment over a wide range of parameters have not yet been made, the essential features of the evolution of an axisymmetric vortex breakdown are evident. The description by Sarpkaya (1971) of the initial axisymmetric swelling of the vortex core together with Escudier's (1986) evolutionary sequence in his Figure 9.12 (reproduced here in Figure 8) are seen in the calculation of the axisymmetric evolution of Figure 6. Noting that in the calculations the time scale of the evolution is given by W_∞/a , and recalling that the Reynolds number is based on the core radius a rather than the pipe diameter, we find that the time scale of the evolution compares favourably, (at a comparable Re) with that obtained in Escudier's (1986) experiment. (Due to the lack of a quantitative measurement in the experiment, only a rough estimate of the core diameter a could be made). A comparison between the structure of the leading bubble with the flow visualizations of Escudier (1986) shows good agreement. For comparable times in both the experiment and the calculation, the bubble migrates upstream approximately the same distance (four bubble diameters) from the point of initial swelling of the core. The appearance of a second breakdown zone at about one bubble diameter downstream from the leading bubble is evident in both experiment and

calculation. In the calculation this second recirculation zone is very unsteady by comparison with the leading bubble and the flow visualization is suggestive of asymmetries in this region of the flow, whereas the leading bubble is evidently largely axisymmetric. Also very evident in the computed leading bubble is the 'two celled' structure first identified in bubble breakdowns by Faler & Leibovich (1978). The main outer cell, or vortex ring, has an associated negative azimuthal component of vorticity and the weaker inner ring has a positive azimuthal component of vorticity.

4. Concluding remarks

Many of the features of vortex breakdown have been well recognised previously. The early works of Benjamin (1962, 1967) have been the starting point for many subsequent studies. However, for the confined flow and the swirling pipe flow, we have not found the 'conjugate flow' theory of particular assistance in illuminating the mechanics of these flows, for the following reasons. The theory assumes a cylindrical flow upstream, whereas in the confined flow, there is no region far upstream of breakdown in which the centrifugal forces balance the radial pressure gradient. Similarly, there is no evidence of the importance of energy dissipation in the outer flow. In the swirling pipe flow case, whereas the 'conjugate flow' theory assumes an inviscid development, the calculations and physical mechanisms for the generation of negative azimuthal vorticity that we have considered depend initially on the diffusion of axial vorticity. It seems nevertheless true that having established breakdown, the azimuthal vorticity which is generated propagates upstream on an inertial time scale and the diffusion of vorticity, which is initially responsible for the breakdown is of lesser significance and continues to operate on the much slower viscous time scale.

From the discussion in this paper, the essential feature of vortex breakdown is the generation of negative azimuthal vorticity. For the confined flow, the rapid generation of this component of vorticity is a consequence of the upstream distribution of $\Gamma(r)$ and $H(r)$ and the non-cylindrical nature of the upstream flow. For the swirling pipe flow, we find the initial reduction in the azimuthal component of vorticity to be due to viscous diffusion and the resultant stretching and tilting of axial vorticity. As the flow begins to diverge however, the further production of negative azimuthal vorticity is dominated by inviscid mechanisms and there is a close similarity between the confined flow and the swirling pipe flow in this region.

A preliminary application of these ideas to the more complex problem of vortex breakdown in delta wing flows suggests that the radial and axial velocity distributions in the core flow which establish a characteristic α_0/β_0 for each angle of attack will play a critical role in determining whether breakdown can occur and if so the strength and location of it. Similarly, by broad analogy with the swirling pipe flow, turbulent diffusion could be expected to be important if the flow initially is in approximate cyclostrophic balance. In this case increased turbulent diffusion would be expected to reduce the size of the breakdown bubble and to reduce the distance to breakdown. Of course, an outer

flow which creates diverging stream surfaces will shorten the distance to breakdown and increase the relative importance of the inviscid mechanism in reducing an initially positive helix angle of the vorticity. [This effect of a diverging outer flow has been observed in swirling pipe flows and may be seen in a comparison between the diverging pipe results of Sarpkaya (1971) and the constant diameter results of Harvey (1962)].

The essential ideas which link the generation of negative azimuthal vorticity with the helix angles of the velocity and vorticity vectors will be applicable also to swirling flows past axisymmetric bodies located on the swirl axis. The positive feedback mechanism could account, for example, for the sensitivity of these flows to the intrusion of external probes leading in some cases to a rapid development of vortex breakdown. For $\alpha_0 > \beta_0$ the divergence of stream surfaces over a body could be expected to lead to a forward recirculation zone ahead of the body if α_0/β_0 is sufficiently large or the body has a large enough diameter. Such a flow with a forward recirculation zone has been observed recently by Joubert (private communication). As discussed in section 2.2, the flow for the case where $\beta_0 > 2\alpha_0$ is much less clear; the negative feedback that would accompany an increase in radius of a stream surface in this case suggests that some dissipative process ahead of the body will occur.

REFERENCES

- Benjamin, T. B. 1962 Theory of the vortex breakdown phenomenon. *J. Fluid Mech.* **14**, 593-629.
- Benjamin, T. B. 1967 Some developments in the theory of vortex breakdown. *J. Fluid Mech.* **28**, 65-84.
- Burgers, J. M. 1940 Application of a model system to illustrate some points of the statistical theory of free turbulence. *Proc. Kon. Ned. Akad. v. Wetensch, Amsterdam XLIII*, 2-12.
- Escudier, M. P. 1986 Lecture 9. Vortex Breakdown in Technology and Nature. in *Von Karman Institute for Fluid Dynamics Lecture Series Programme. 10. Introduction to Vortex Dynamics. May 1986*.
- Escudier, M. P.; Bornstein, J. & Zehnder, N. 1980 Observations and LDA measurements of confined turbulent vortex flow. *J. Fluid Mech.* **98**, 49-63.
- Faler, J. H. & Leibovich, S. 1978 An experimental map of the internal structure of a vortex breakdown. *J. Fluid Mech.* **86**, 313-335.
- Garg, A. K. & Leibovich, S. 1979 Spectral characteristics of vortex breakdown flowfields. *Phys. Fluids* **22**, 2053-2064.
- Harvey, J. K. 1962 Some observations of the vortex breakdown phenomenon. *J. Fluid Mech.* **14**, 585-592.
- Joubert, P. N. 1987 University of Melbourne. *Private communication*.
- Lopez, J. M. 1986 Numerical simulation of axisymmetric vortex breakdown *Proc. 9th Australasian Fluid Mech. Conf., Univ. of Auckland, New Zealand*.
- Lopez, J. M. 1988 Axisymmetric vortex breakdown. Part I: Confined swirling flow *J. Fluid Mech.* , submitted with this paper (also available as A.R.L. Aero. Report 173 AR-004-572).
- Squire, H.B. 1960 Analysis of the 'vortex breakdown' phenomenon. Part I. *Imperial College of Science and Technology, Aeronautics Department Report No. 102*.
- Sarpkaya, T. 1971 Vortex breakdown in swirling conical flows. *AIAA J.* **9**, 1792-1799.
- Uchida, S.; Nakamura, Y. & Ohsawa, M. 1985 Experiments on the axisymmetric vortex breakdown in a swirling air flow. *Trans. Japan Soc. Aero. Space Sci.* **27**, 206-216.

Appendix I

The main difficulty in the numerical solution of the swirling pipe flow vortex breakdown problem lies in the specification of the boundary conditions. The boundary condition on the axis of symmetry is obvious but the other three boundary conditions require a higher level of idealization.

The upstream boundary condition at $z = 0$ is the one of main concern. Due to the limited number of available grid nodes (a 101×501 grid has been an upper limit in this calculation) the swirl generator, i.e. guide vanes, and the pipe inlet could not be simulated at the same time as the flow inside the pipe 'test-section'. Hence, the upstream boundary must be placed at some location downstream of the inlet and upstream of the 'test-section'. This requires an assumption that the flow at the upstream boundary is locally cylindrical and independent of time throughout the evolution of the calculated flow. Over the past decade, there have been numerous Laser Doppler Anemometer measurements of the azimuthal and axial components of the velocity (eg. Faler & Leibovich (1978), Escudier, Bornstein & Zehnder (1980), Uchida, Nakamura & Ohsawa (1985)) and it has been found that the expressions (16) and (17) provide a good fit to the experimental distributions well upstream of the location where vortex breakdown occurs. For those numerical cases where vortex breakdown first appears well downstream of the inlet it would seem therefore that these expressions, used as boundary conditions, are a reasonable approximation.

In those cases where the breakdown bubble migrates upstream a change in the velocities near the upstream boundary as a result of this migration is a clear indication that the numerical flow has become 'unphysical'. In many cases there is a substantial evolution of the 'breakdown' before this occurs. The weakness in this boundary condition requiring further evaluation, however, is that the viscosity changes discontinuously at the boundary and correspondingly gradients in v (and therefore u) change relatively rapidly at low Reynolds number, near the boundary.

Of lesser importance, but with its own problems, is the specification of the radial and downstream boundary conditions. At the downstream boundary, the usual uniform outflow condition is specified. In the numerical experiments performed, so long as no rotational flow enters into the computational domain through this boundary, changes in the location of this boundary demonstrated that the effect of the downstream boundary was negligible in these calculations, in the development of the initial breakdown. How-

ever, under some conditions, it was found that multiple recirculation bubbles formed (much like those reported by Sarpkaya (1971)) and when a bubble forms very near the downstream boundary (which often happens when the initial azimuthal component of vorticity is large and positive as a result of a strong axial jet), then the assumption of uniform outflow is clearly violated and the calculation becomes unphysical. A crude remedy used was to extend the computational domain further downstream.

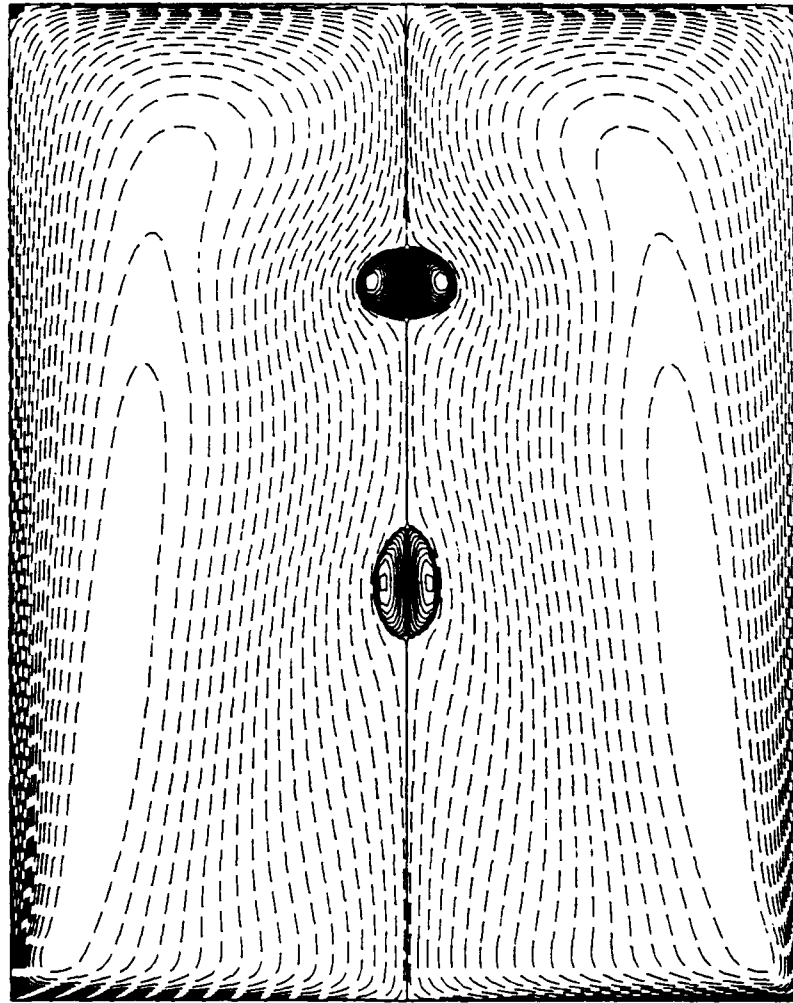
The radial boundary condition is a somewhat less difficult problem. Typically, it was found that if the radial boundary is placed at a radius of at least two core diameters, then the numerical evolution is weakly affected by this boundary. A similar weak influence of the radial boundary was also found in the experiments of Harvey (1962). In the model, the computational domain is stretched in the radial direction so that there is a concentration of grid nodes near $r = 0$ thus allowing proper resolution of the dynamics in the core region. The radial boundary condition is taken to simulate a limiting streamline, in the irrotational region of the flow, which remains parallel to the pipe wall. This is physically reasonable so long as the diffusion of vorticity is not large enough to invalidate the irrotational approximation and the boundary layer on the pipe wall (which is not computed) remains thin and attached.

An interesting and relevant observation to be made is the difference between the 'downstream' boundary condition in the confined swirling flow case and that in other flows in which vortex breakdown occurs. In these other cases (e.g. vortical flow over delta winged aircraft, swirling pipe flows, Ward-type cyclone chambers, tornados and waterspouts) the downstream boundary condition on the vortex core is 'free', whereas in the confined swirling flow the rotating endwall forms the downstream boundary which results in the physical boundary condition that $v = 0$ at $r = 0$. The vortex core is therefore fixed to the center of the downstream boundary. Having this fixed downstream boundary condition on the vortex core accounts perhaps for the fact that the 'spiral' form of vortex breakdown which is evident in the other examples of vortex breakdown is not evident at the values of $\Omega R^2/\nu$ and H/R reported in the confined flow experiments.

Re	λ (eq. 15)	λ (eq. 14)	λ (num. soln.)
1600	0.64	0.87	1.03
1800	0.55	0.81	0.82
1918	0.57	0.72	0.77
1942	0.70	0.72	0.77
1994	0.66	0.72	0.77
2126	0.61	0.69	0.75
2494	0.66	0.61	0.72

TABLE 1: ESTIMATES OF THE WAVELENGTHS OF THE OSCILLATIONS IN THE DISPLACEMENT OF THE STREAMSURFACE DETERMINED (i) FROM THE EXPRESSION GIVEN BY (15) AND (ii) FROM THE PERIODICITY IN THE CONTOURS OF $v^2/r - 1/\rho \partial p / \partial r$ FOR VARIOUS Re AS INDICATED AND $H/R = 2.5$.

(a) Ψ : $Re = 1994$ $H/R = 2.5$

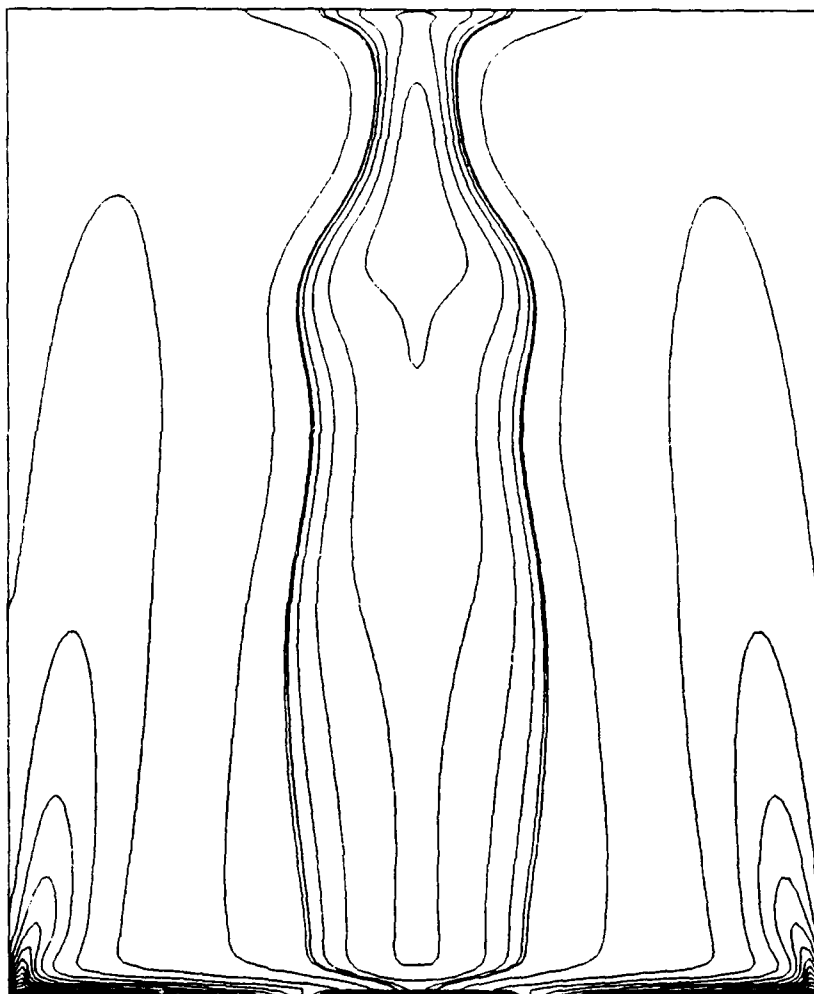


min. $= -7.8 \times 10^{-3}$

max. $= 8.8 \times 10^{-6}$

FIGURE 1: CONTOURS OF (a) ψ , (b) Γ AND (c) H IN THE MERIDIONAL PLANE FOR $H/R = 2.5$ AND $Re = 1994$. THE CONTOUR LEVELS ARE NON-UNIFORMLY SPACED, WITH 20 POSITIVE AND 20 NEGATIVE LEVELS DETERMINED BY $c\text{-LEVEL}(i) = \text{MAX}(\text{variable}) + (i/20)^{\text{ind}}$ AND $c\text{-LEVEL}(i) = \text{Min}(\text{variable}) \times (i/20)^{\text{ind}}$ RESPECTIVELY, WHERE $\text{ind} = 3$ IN (a) & (b) AND $\text{ind} = 2$ IN (c). THE CONTOURS ARE PLOTTED AT $t = 1000$, BY WHICH TIME A STEADY STATE HAS BEEN REACHED.

(c) H: $Re = 1994$ $H/R = 2.5$

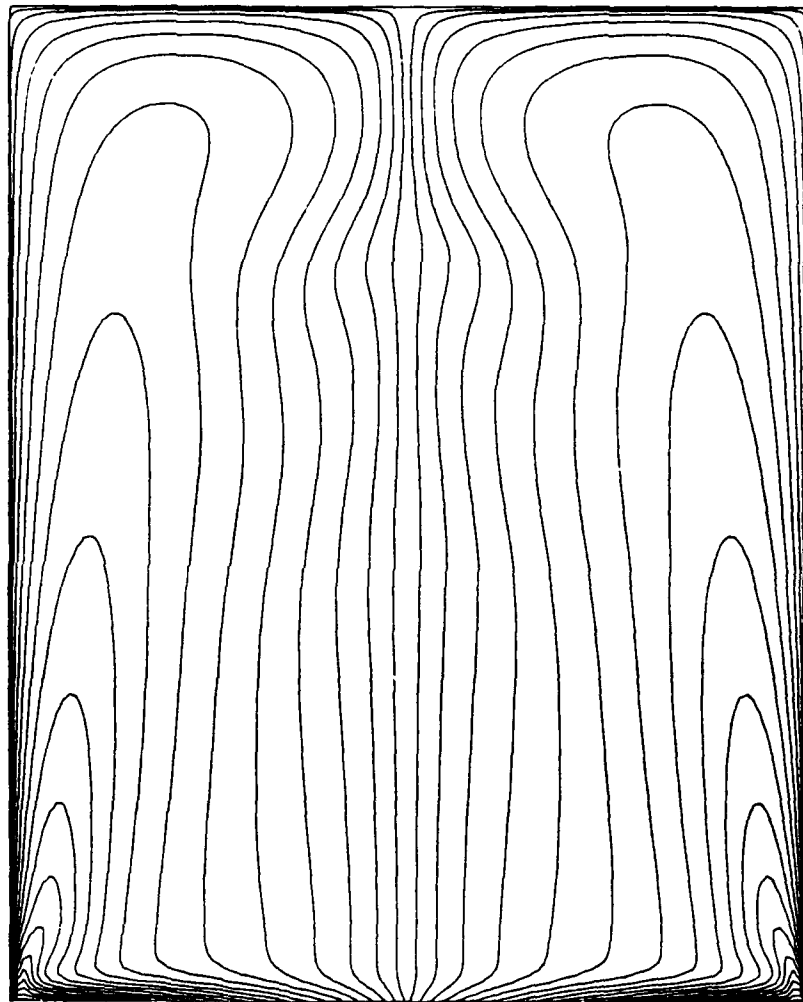


min. $= -3.8 \times 10^{-2}$

max. $= 6.5 \times 10^{-1}$

FIGURE 1c

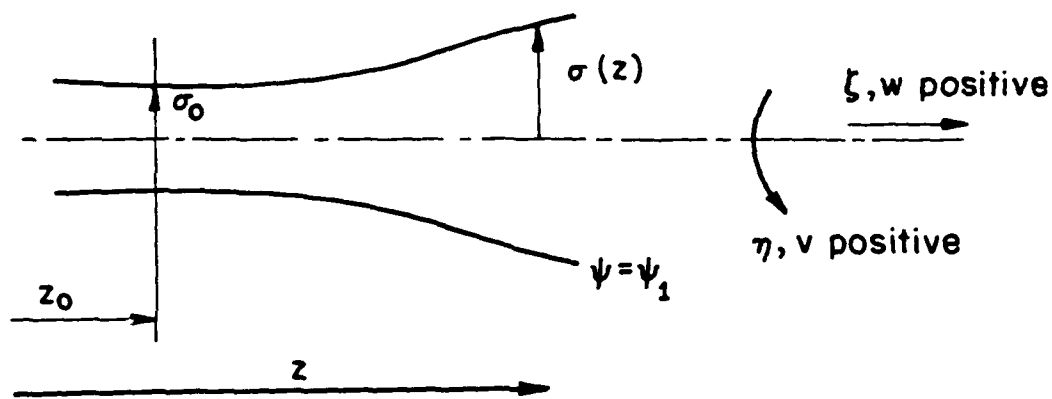
(b) Γ : $Re = 1994$ $H/R = 2.5$



min. = 0

max. = 1.0

FIGURE 1b



at $z = z_0$ $r = \sigma_0$ (if $\frac{\partial u}{\partial z} = 0$ then $\eta_0 = -\frac{\partial w}{\partial r} \bigg|_{\sigma_0}$)

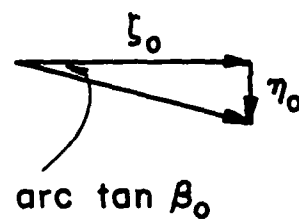
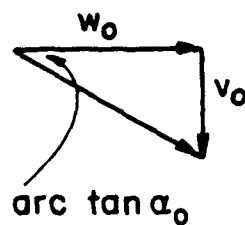
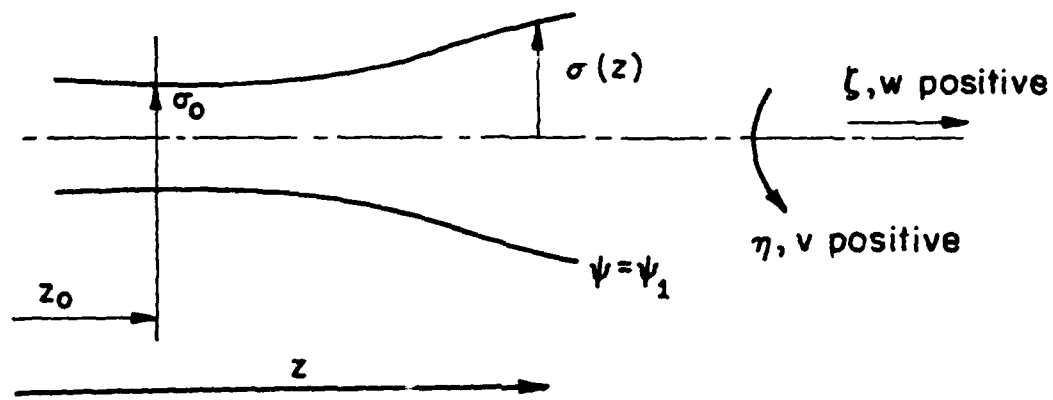


FIGURE 2: CO-ORDINATE SYSTEM USED AND A TYPICAL STREAM SURFACE $\psi = \psi_1$ FOR WHICH $r = \sigma(z)$ AND THE HELIX ANGLES FOR THE VELOCITY AND VORTICITY AT z_0 ARE α_0 AND β_0 .



at $z = z_0$ $r = \sigma_0$ (if $\frac{\partial u}{\partial z} = 0$ then $\eta_0 = -\frac{\partial w}{\partial r}\bigg|_{\sigma_0}$)

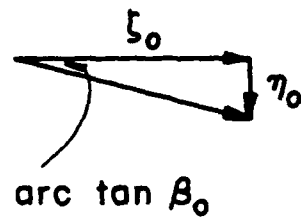
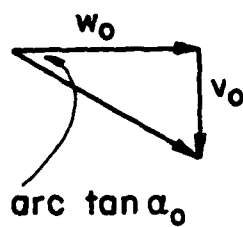
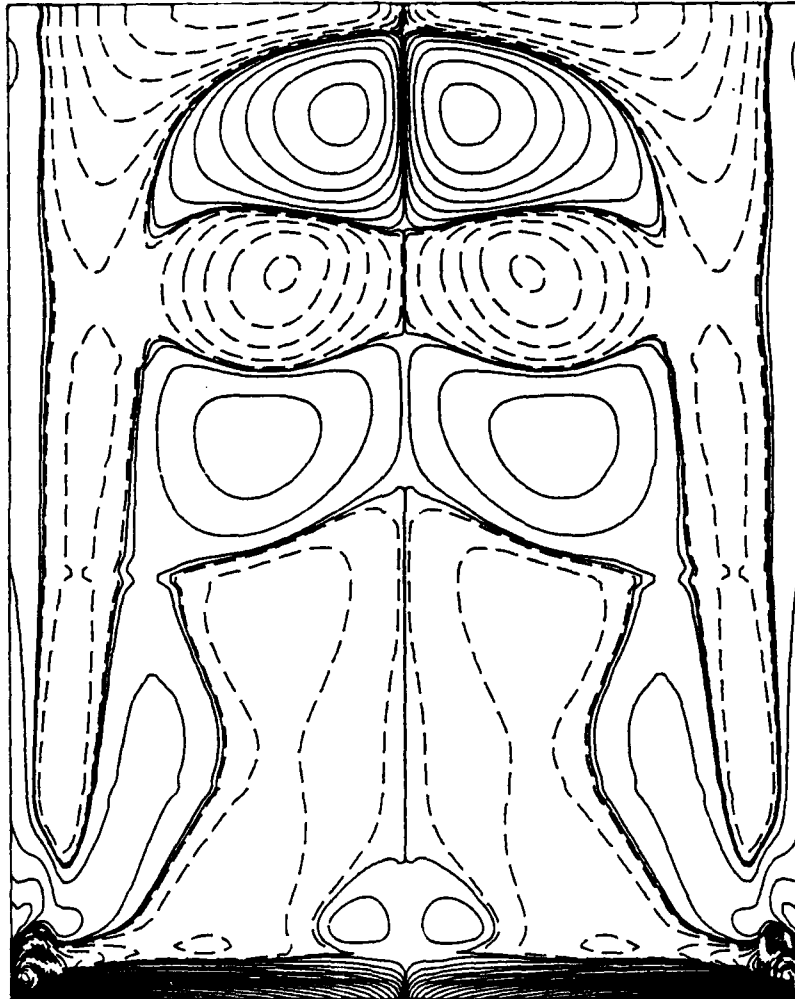


FIGURE 2: CO-ORDINATE SYSTEM USED AND A TYPICAL STREAM SURFACE $\psi = \psi_1$ FOR WHICH $r = \sigma(z)$ AND THE HELIX ANGLES FOR THE VELOCITY AND VORTICITY AT z_0 ARE α_0 AND β_0 .

Re=1994 H/R=2.5

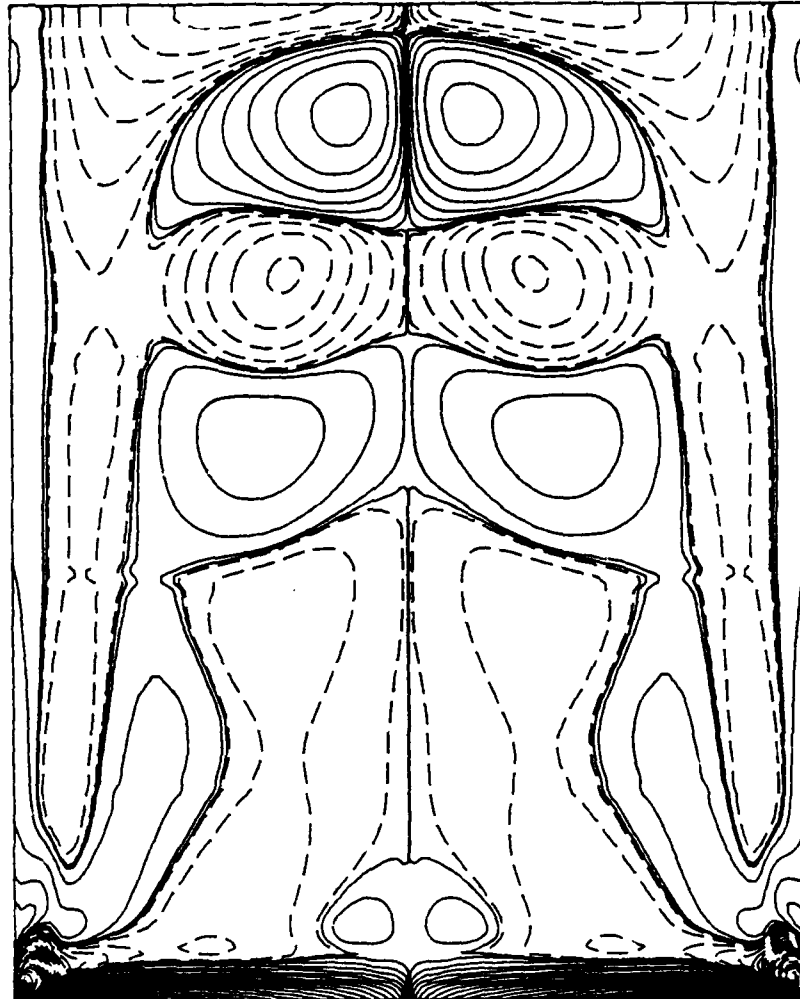


min.=0.19

max.=0.33

FIGURE 4: CONTOUR PLOT OF $v^2/r - 1/\rho \partial p / \partial r$ IN THE MERIDIONAL PLANE FOR $H/R = 2.5$ AND $Re = 1994$. THE CONTOUR LEVELS ARE NON-UNIFORMLY SPACED, WITH 20 POSITIVE AND 20 NEGATIVE LEVELS DETERMINED BY $C\text{-LEVEL}(i) = \text{MAX}(\text{variable}) \times (i/20)^3$ AND $C\text{-LEVEL}(i) = \text{MIN}(\text{variable}) \times (i/20)^3$ RESPECTIVELY. THE CONTOURS ARE PLOTTED AT $t = 1000$, BY WHICH TIME A STEADY STATE HAS BEEN REACHED.

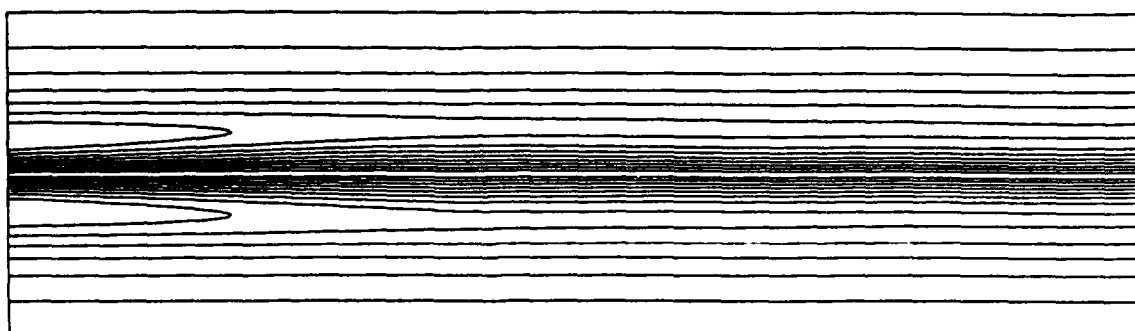
Re=1994 H/R=2.5



min.=0.19

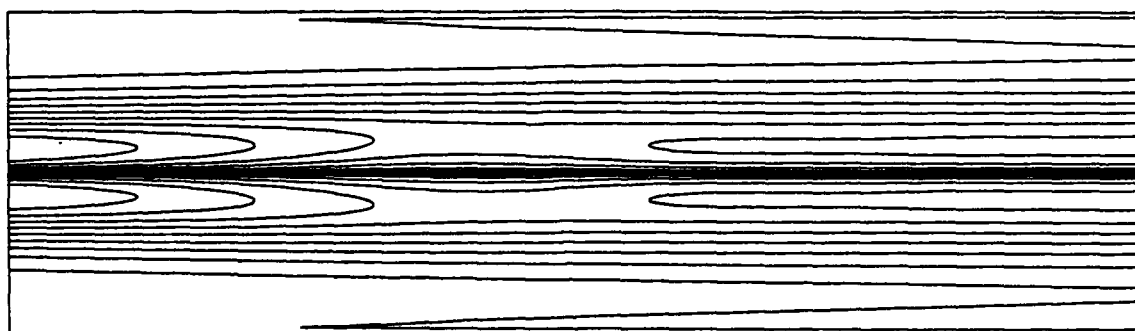
max.=0.33

FIGURE 4: CONTOUR PLOT OF $v^2/r - 1/\rho \partial p / \partial r$ IN THE MERIDIONAL PLANE FOR $H/R = 2.5$ AND $Re = 1994$. THE CONTOUR LEVELS ARE NON-UNIFORMLY SPACED, WITH 20 POSITIVE AND 20 NEGATIVE LEVELS DETERMINED BY $C\text{-LEVEL}(i) = \text{MAX}(\text{variable}) \times (i/20)^3$ AND $C\text{-LEVEL}(i) = \text{MIN}(\text{variable}) \times (i/20)^3$ RESPECTIVELY. THE CONTOURS ARE PLOTTED AT $t = 1000$, BY WHICH TIME A STEADY STATE HAS BEEN REACHED.



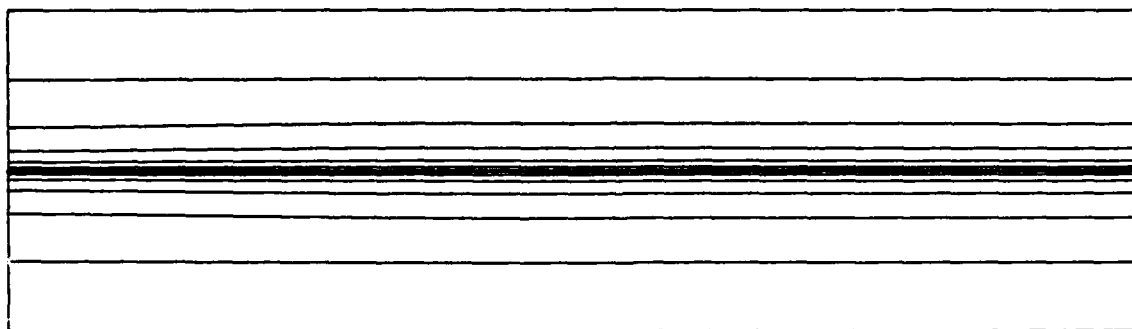
min.=0

max.=1.51410281



min.=0

max.=1.07213902



min.=0

max. 13.125

FIGURE 6(ii) $t=40$

FIGURE 6(i) $t=20$

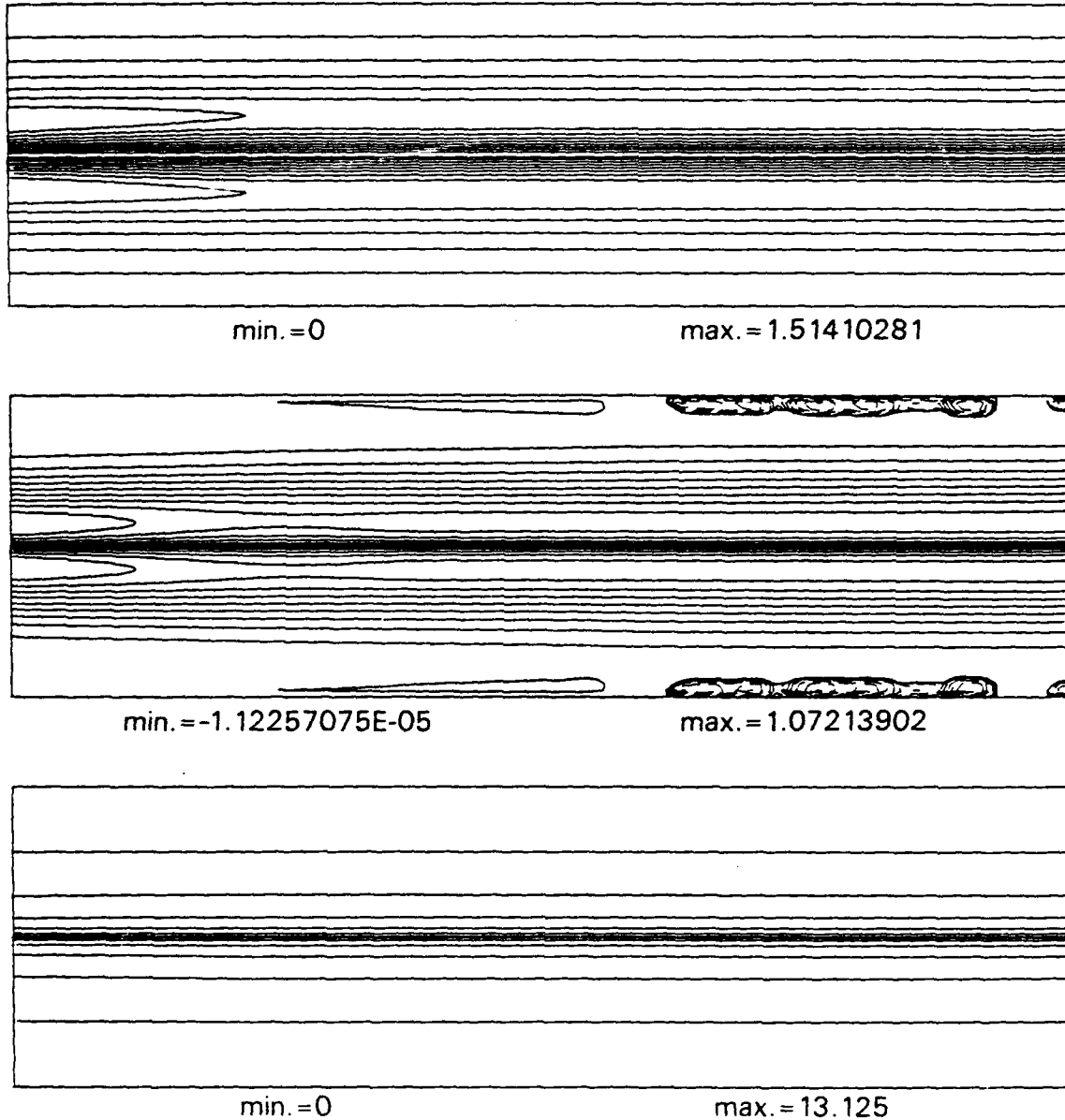
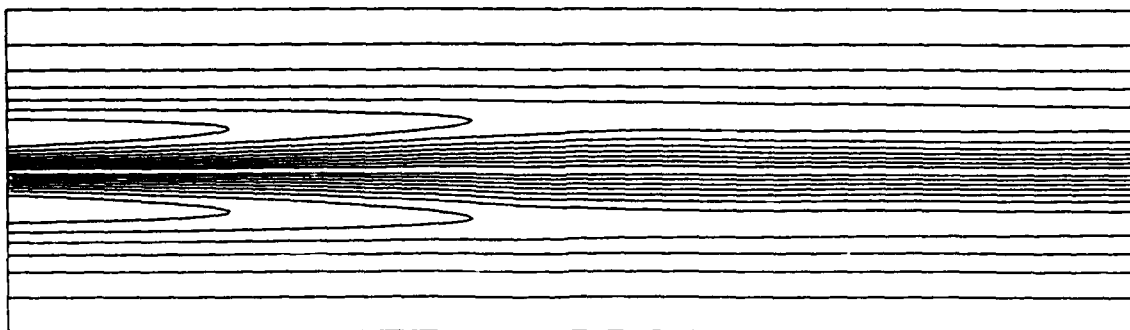
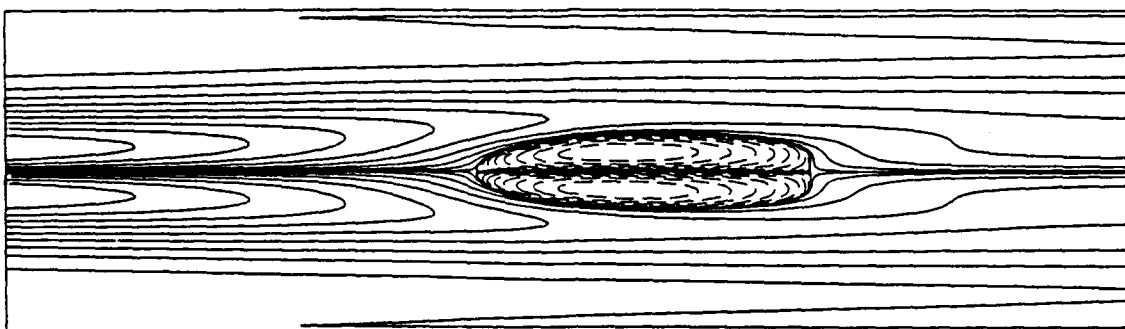


FIGURE 6: THE EVOLUTION OF THE AXISYMMETRIC VORTEX BREAKDOWN PHENOMENON IN SWIRLING PIPE FLOW FOR THE CASE OF $V_c = 1.5$, $W_c = 1.25$ AND $Re = W$, $a/r = 250$. THE COMPUTATIONAL DOMAIN HAS A RADIAL EXTENT OF $5a$ AND AN AXIAL EXTENT OF $35a$ IN WHICH 351 GRID POINTS ARE UNIFORMLY DISTRIBUTED IN THE AXIAL DIRECTION AND 51 GRID POINTS ARE NON-UNIFORMLY DISTRIBUTED IN THE RADIAL DIRECTION AND ARE CONCENTRATED NEAR $r = 0$. THE TIME INCREMENT FOR THE EVOLUTION IS $\delta t = 0.01$ AND THE NON-DIMENSIONAL TIMES AT WHICH THE CONTOURS OF (i) v , (ii) η AND (iii) ψ HAVE BEEN PLOTTED, ARE INDICATED IN EACH FIGURE.



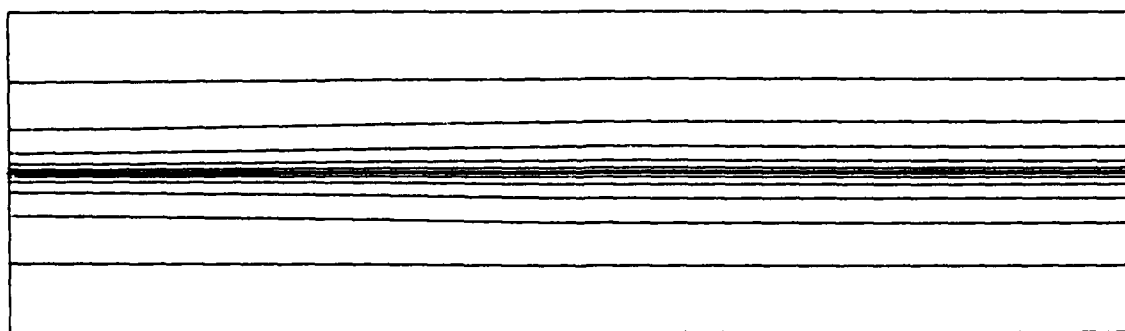
min.=0

max.= 1.51410281



min.=-0.108444847

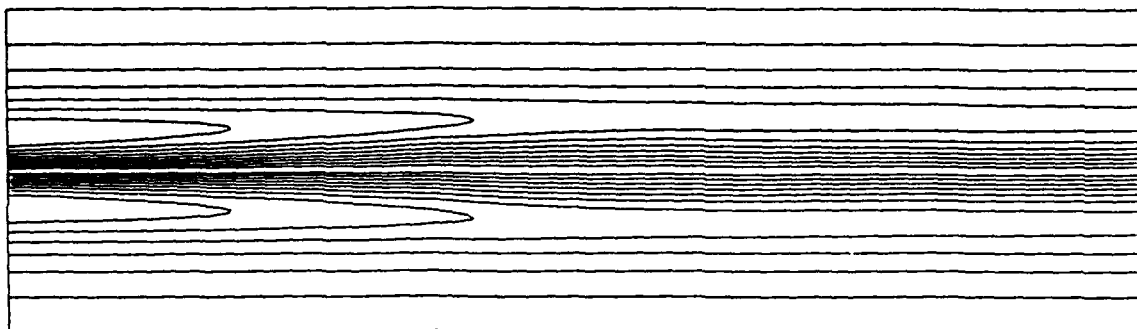
max.= 1.07213902



min.=0

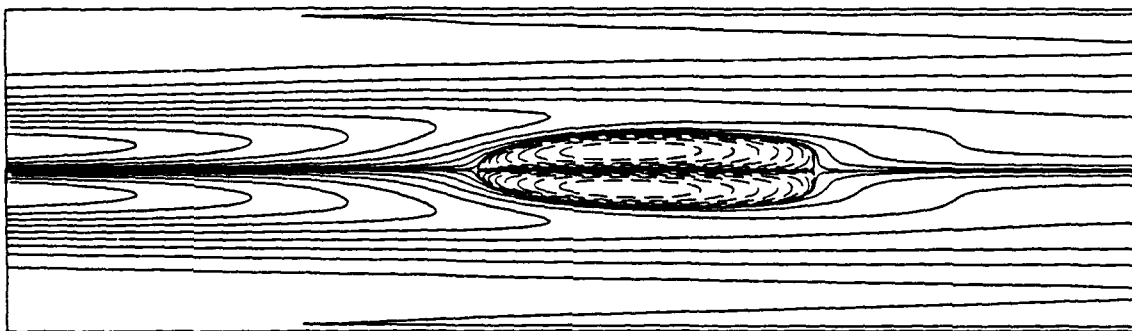
max.13.125

FIGURE 6 (iv) $t=80$



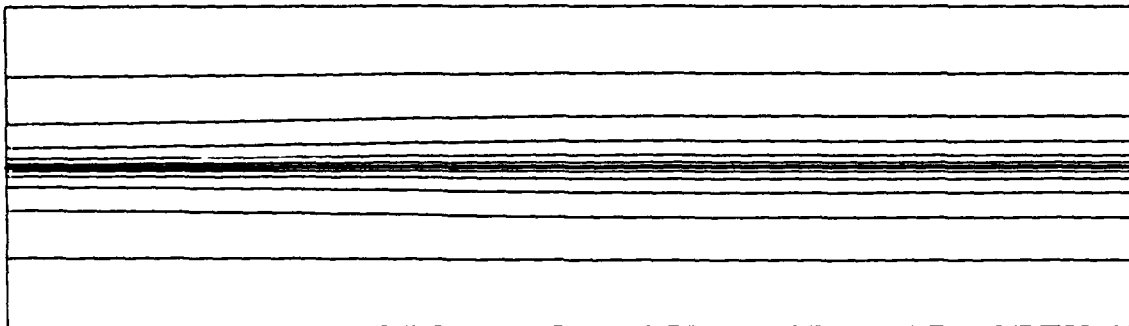
min.=0

max.=1.51410281



min.=-0.108444847

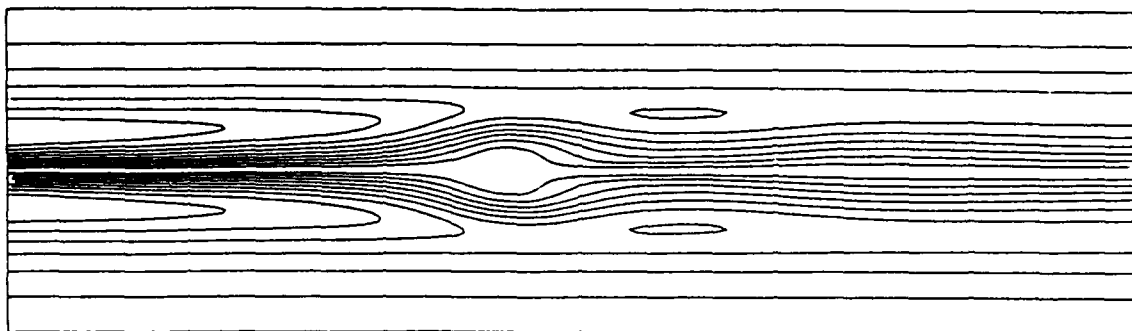
max.=1.07213902



min.=0

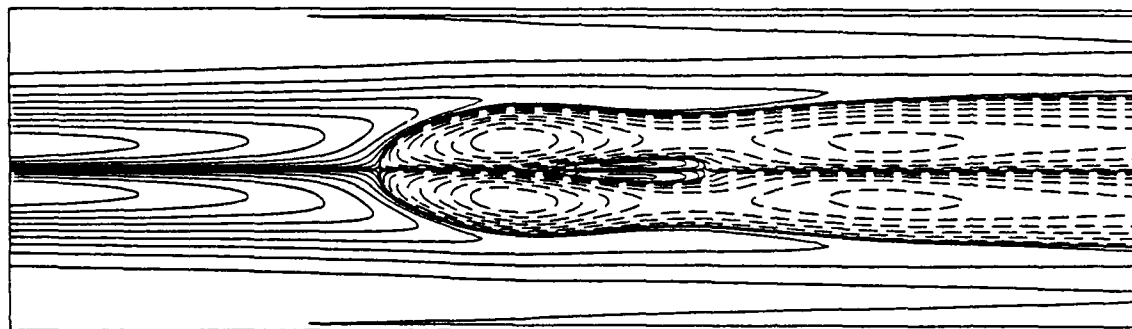
max.13.125

FIGURE 6 (iv) $t=80$



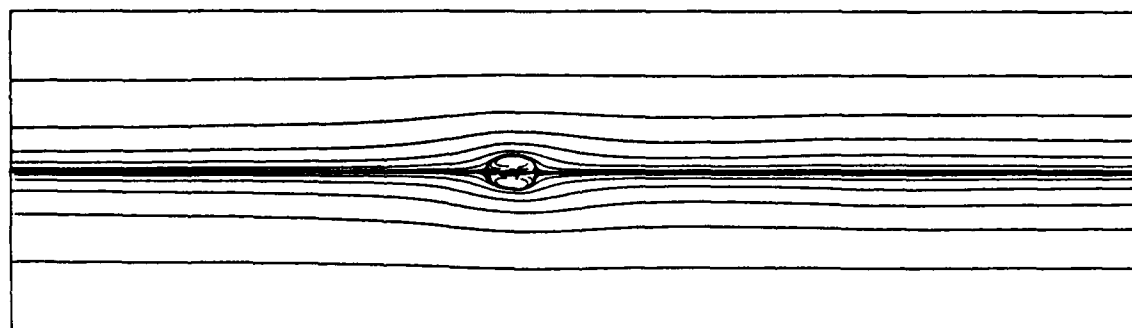
min. = 0

max. = 1.51410281



min. = -1.33221864

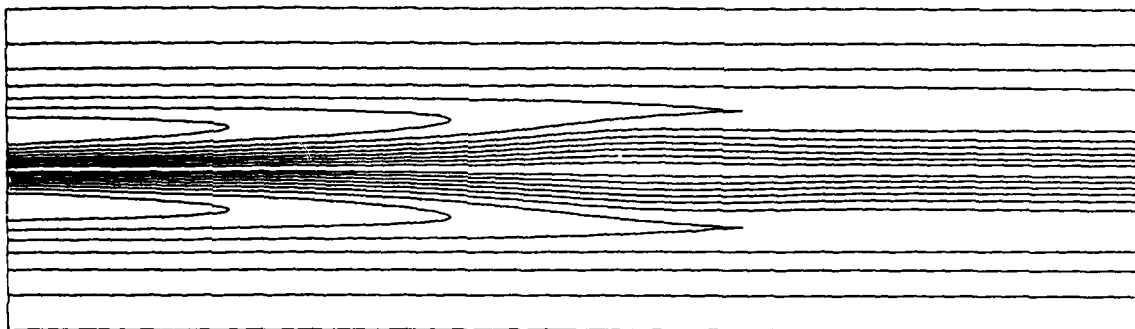
max. = 1.07213902



min. = -4.13780473E-03

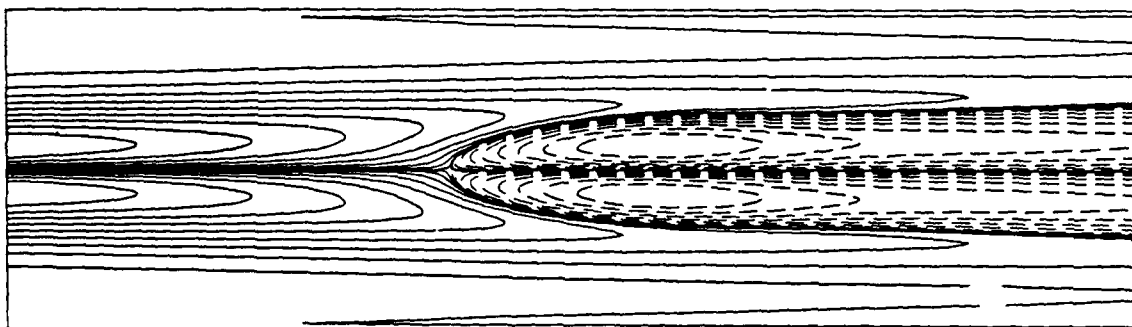
max. = 13.125

FIGURE 6 (vi) $t=240$



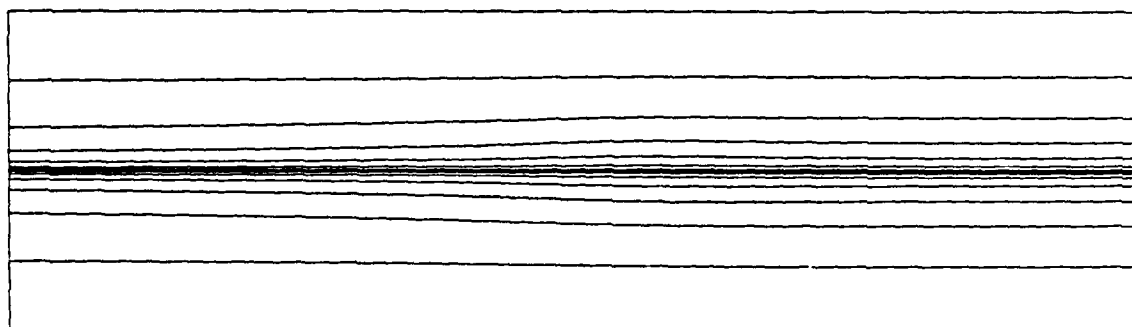
min. = 0

max. = 1.51410281



min. = -0.467498779

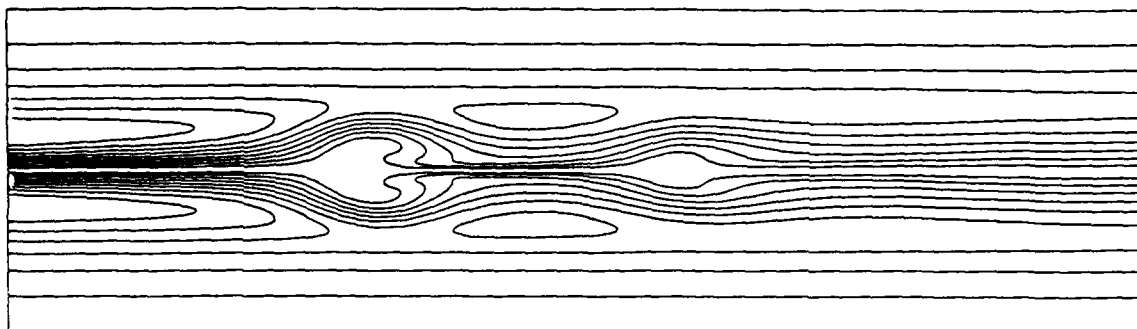
max. = 1.07213902



min. = 0

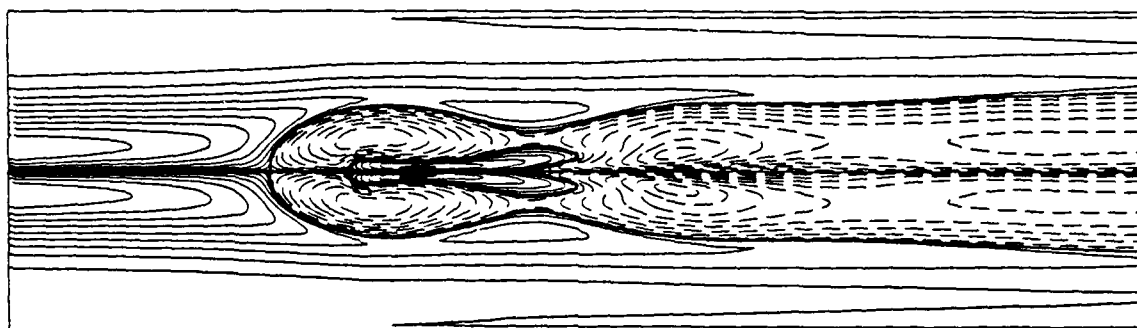
max. = 13.125

FIGURE 6 (v) $t=140$



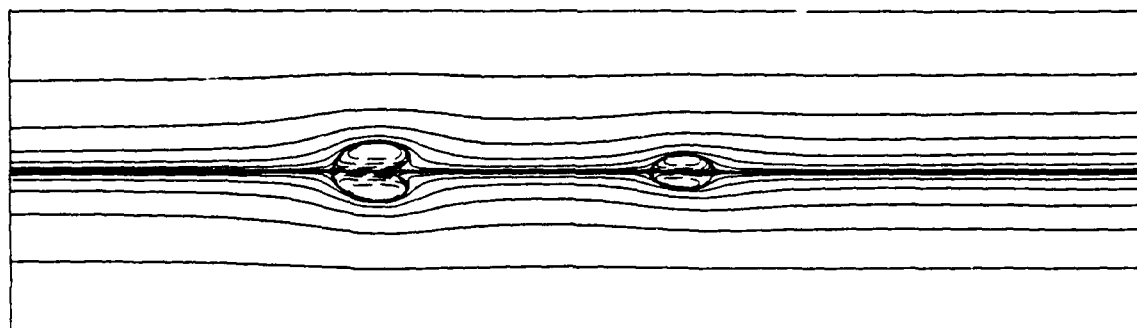
min. = 0

max. ≈ 1.51410281



min. = -1.84688413

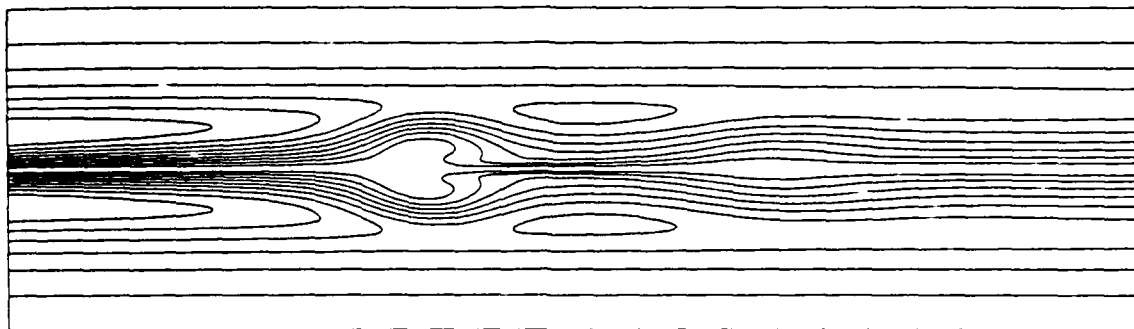
max. = 1.07213902



min. = -2.52486914E-02

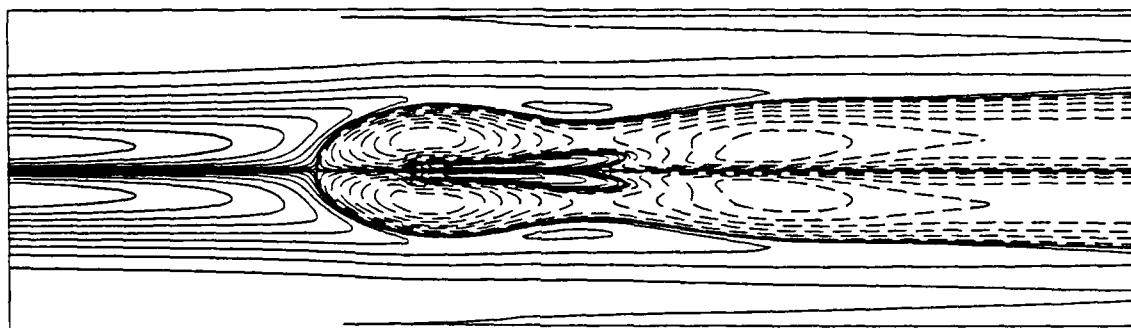
max. = 13.125

FIGURE 6 (viii) $t=310$



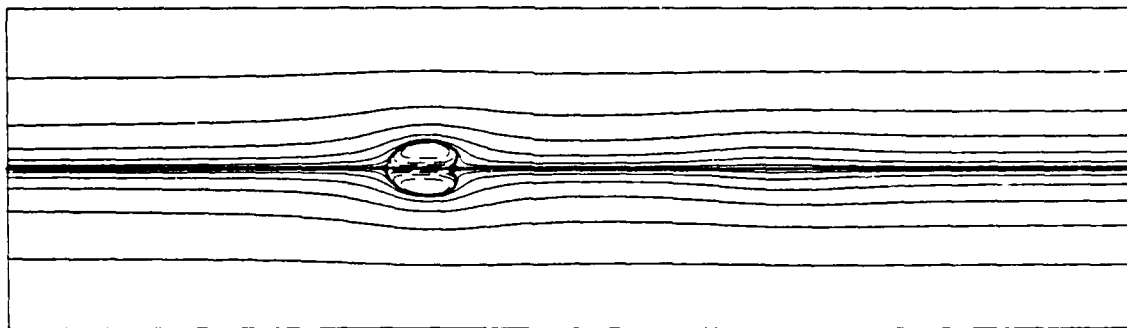
min. = 0

max. = 1.51410281



min. = -1.68802809

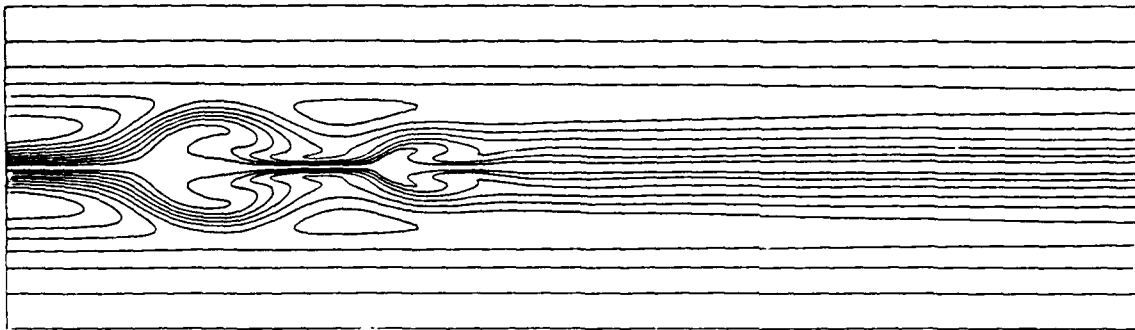
max. = 1.07213902



min. = -2.11477149E-02

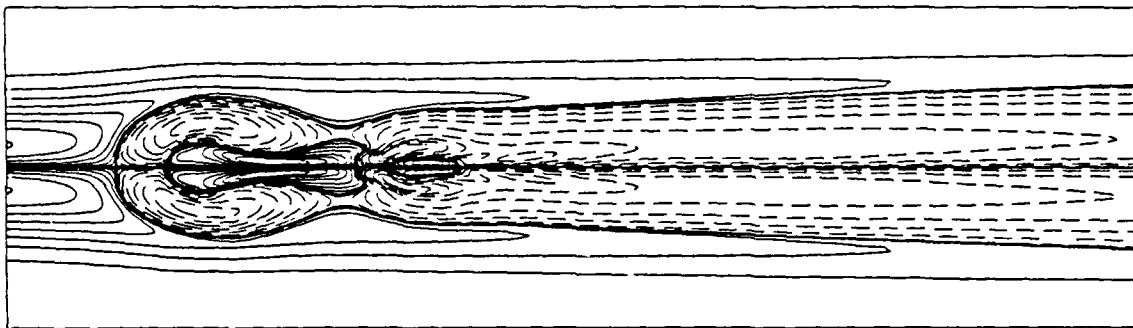
max. 13.125

FIGURE 6 (vii) $t=280$



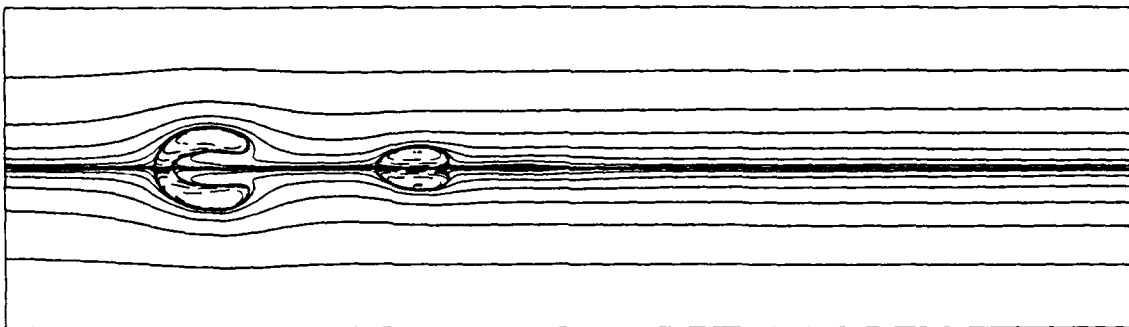
min.=0

max.=1.51410281



min.=-3.76317954

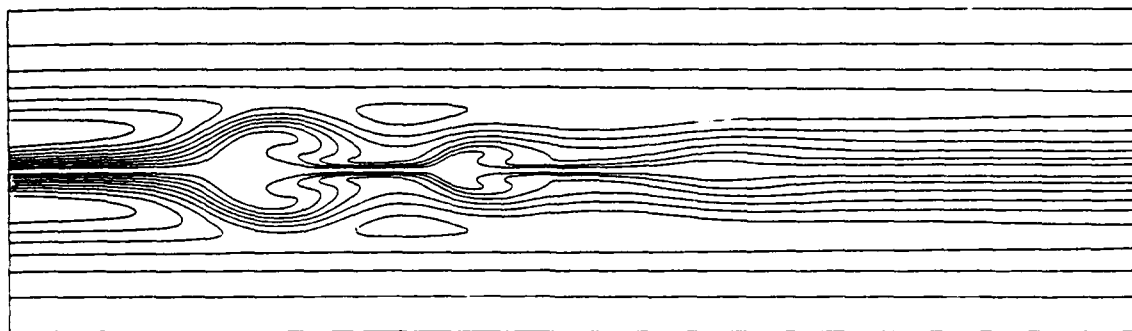
max.=2.03598761



min.=-5.33931851E-02

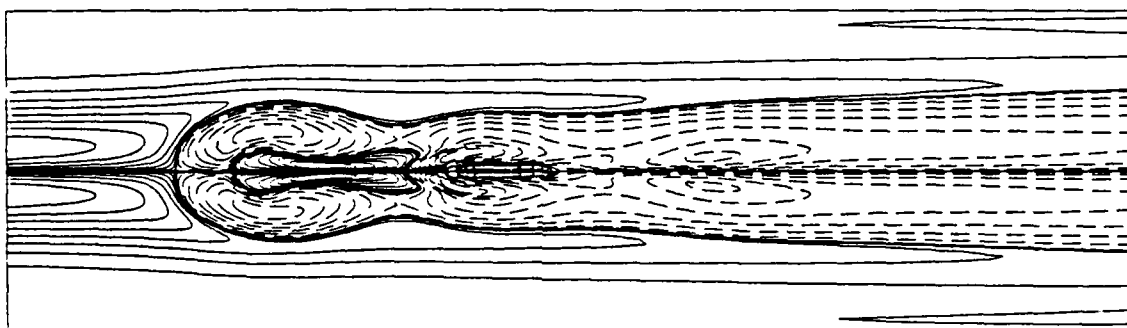
max.=13.125

FIGURE 6 (x) $t=416$



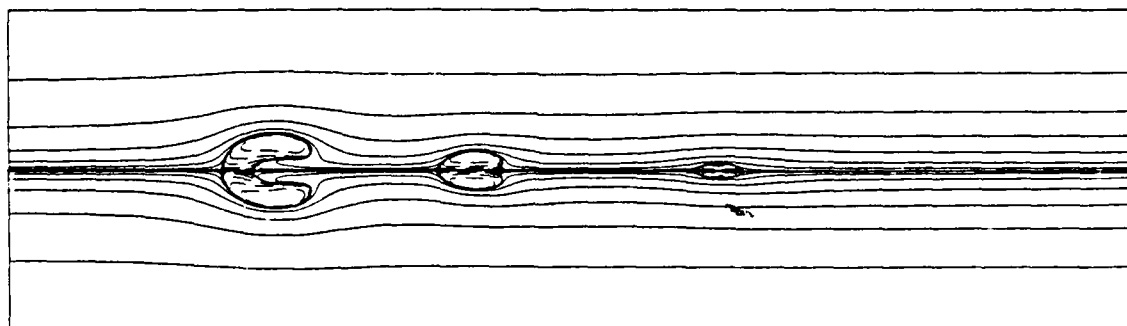
min. = 0

max. = 1.51410281



min. = -3.3361721

max. = 1.5793389



min. = -4.40779142E-02

max. = 13.125

FIGURE 6 (ix) $t=376$

FIGURE 7: CALCULATED CONTOURS OF (i) ψ , (ii) η AND (iii) v FOR A FLOW WITH $V_c = 1.75$, $W_c = 1.6$ AND Re INITIALLY 300. (THE COMPUTATIONAL DOMAIN IS OF RADIAL EXTENT 4a AND AXIAL EXTENT 36a WITH 361 UNIFORMLY DISTRIBUTED GRID NODES IN THE AXIAL DIRECTION AND 41 NON-UNIFORMLY DISTRIBUTED GRID NODES IN THE RADIAL DIRECTION. THE TIME INCREMENT USED IS $\delta t = 0.01$.) (a) $t = 227$ AND $Re = 300$; (b) $t = 250$ AND $Re = 300$; (c) $t = 250$ FOLLOWING A REDUCTION AT $t = 227$ IN Re FROM 300 TO 150; (d) $t = 250$ FOLLOWING AN INCREASE AT $t = 227$ IN THE Re FROM 300 TO 600.

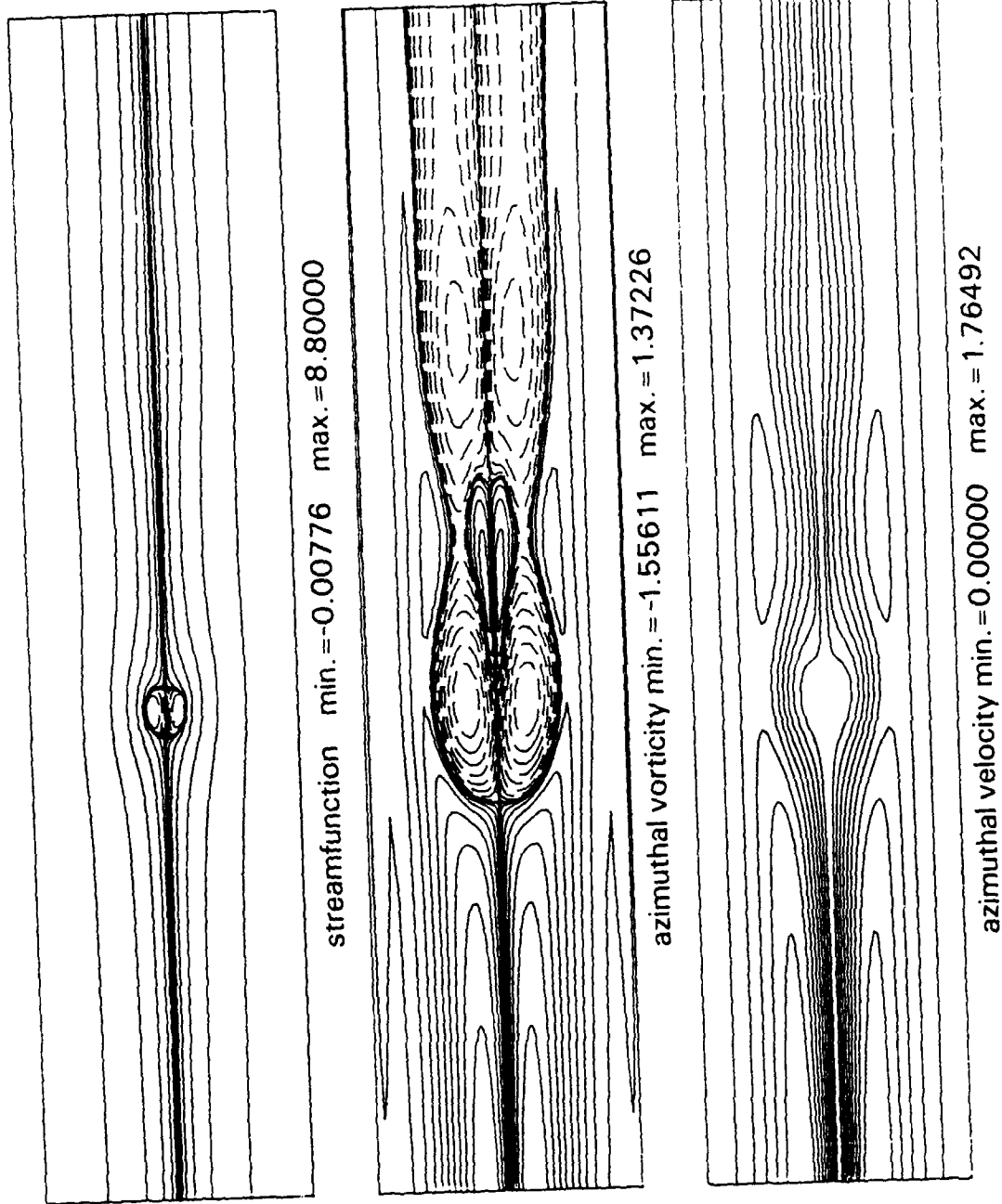
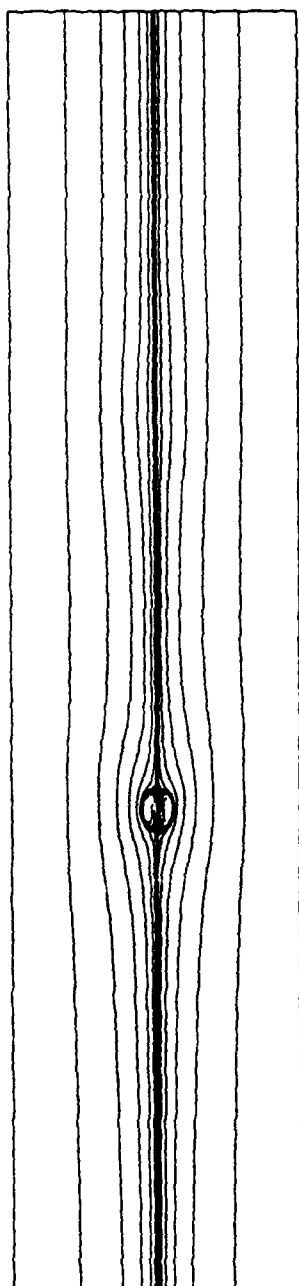
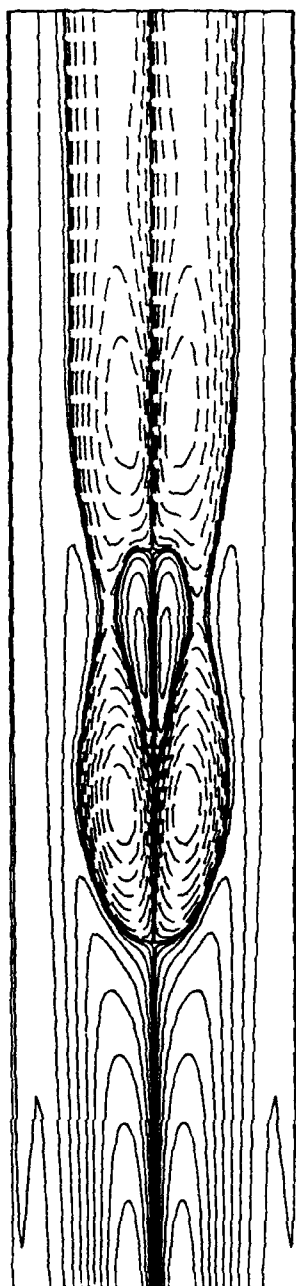


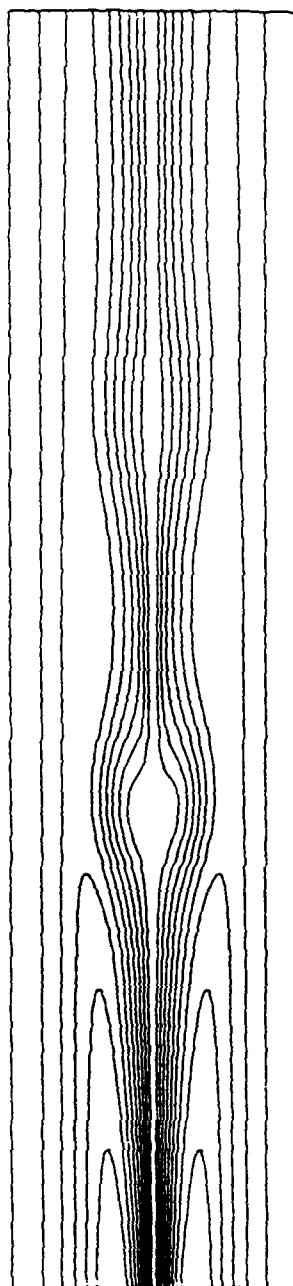
FIGURE 7 (a) $Re=300$, $t=227$



streamfunction min. = -0.00233 max. = 8.80000

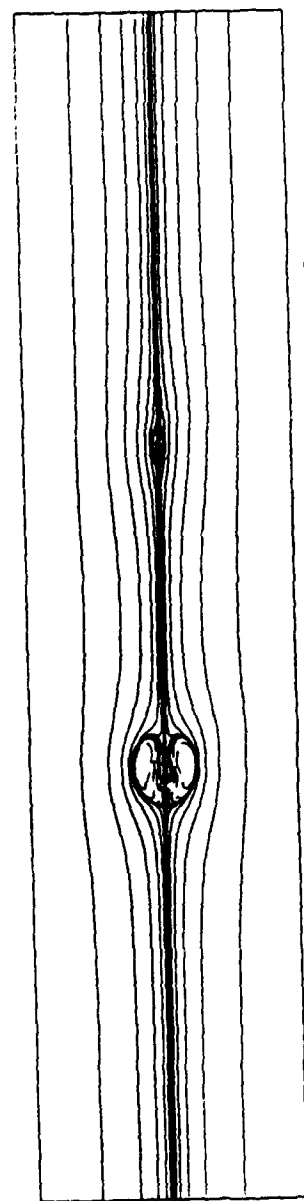


azimuthal vorticity min. = -1.37337 max. = 1.37226

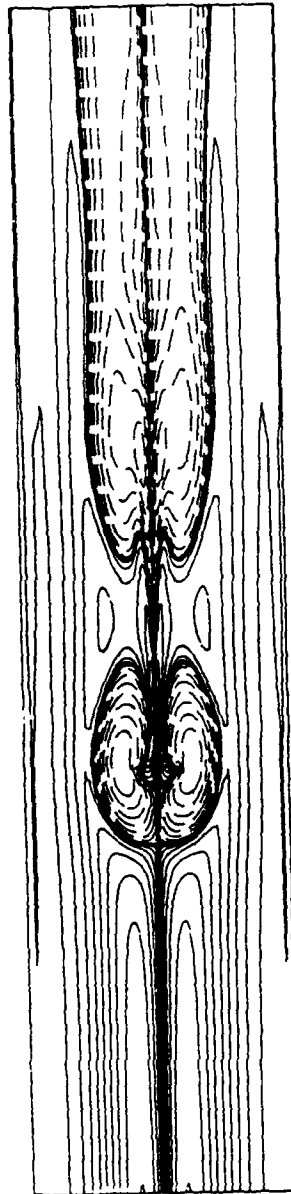


azimuthal velocity min. = 0.00000 max. = 1.76492

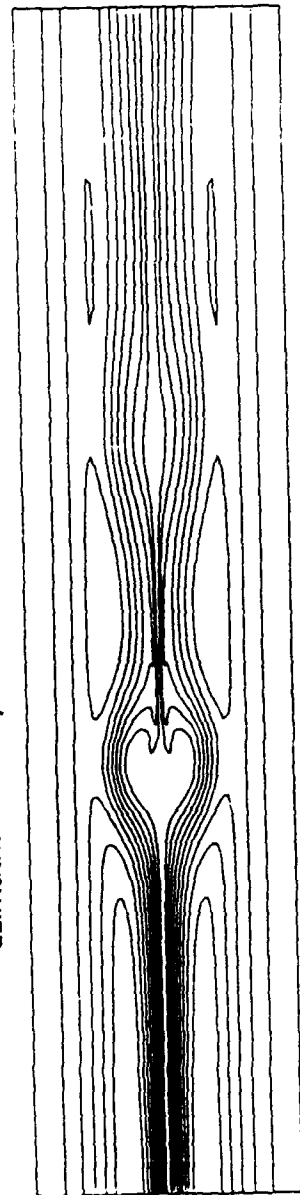
FIGURE 7 (c) $Re = 150$, $t = 250$



streamfunction min. = -0.03738 max. = 8.80000



azimuthal vorticity min. = -2.17319 max. = 1.86395



azimuthal velocity min. = 0.00000 max. = 1.76492

FIGURE 7 (d) $Re=600$, $t=250$

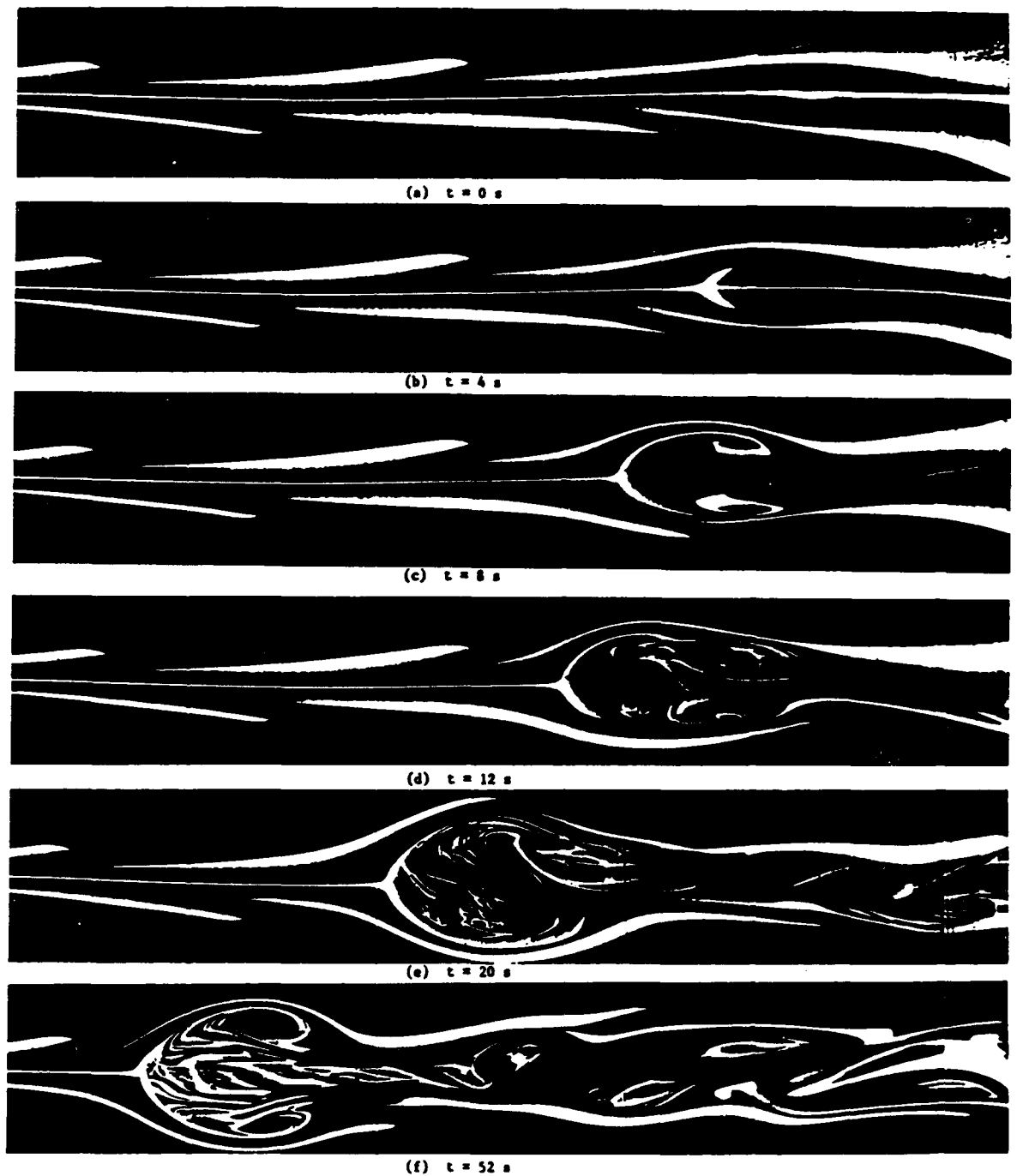


FIGURE 8: ESCUDIER'S (1986) OBSERVATION OF THE FORMATION AND PROPAGATION OF AN AXISYMMETRIC (BUBBLE TYPE) VORTEX BREAKDOWN DOWNSTREAM OF A GUIDEVANE SYSTEM, (VANE ANGLE $\phi = 70^\circ$ AND THE REYNOLDS NUMBER, BASED ON THE PIPE DIAMETER AND MEAN AXIAL VELOCITY, IS 960.)

UNITED STATES OF AMERICA

NASA Scientific and Technical Information Facility
Director NASA Langley, Mr R.H. Peterson
Director NASA Lewis, Dr J.M. Klineberg
Director NASA Ames, Dr W.F. Ballhaus, Jr.
Boeing Company, Library
United Technologies Corporation, Library
Lockheed-California Company
Lockheed Missiles and Space Company
Lockheed Georgia
McDonnell Aircraft Company, Library
McDonald Douglas Research Laboratory, Director

Universities and Colleges

Massachusetts Inst. of Technology
Professor M.T. Landahl

CALTECH

Professor P.G. Saffman
Professor H.G. Hornung
Professor A. Roshko

Cornell

Professor S. Leibovich

Stanford

Professor W.C. Reynolds
Professor S.J. Kline
Professor B.J. Cantwell

Naval Post-Graduate School
Professor T. Sarpkaya

University of South Carolina
Professor T. Maxworthy

Spares (20 copies)
TOTAL (122 copies)

Universities and Colleges

Toronto

Institute for Aerospace Studies

FRANCE

ONERA, Library

GERMANY

Institute für Stromungsmechanik der DFVLR, Professor H. Ludwig

INDIA

National Aeronautical Laboratory,
Professor R. Nasasimha (Director)

ISRAEL

Technion-Israel Institute of Technology
Professor J. Singer

JAPAN

National Aerospace Laboratory

NETHERLANDS

National Aerospace Laboratory (NLR), Library

SWEDEN

Aeronautical Research Institute, Library

SWITZERLAND

Brown, Boveri, and Co., Dr J.J. Keller

UNITED KINGDOM

Royal Aircraft Establishment, Farnborough

Director, Dr G.G. Pope,

Dr M.G. Hall

British Aerospace

Kingston-upon-Thames, Library

Schlumberger Cambridge Research Ltd., Dr M.P. Escudier

Universities and Colleges

Cambridge

Professor G.K. Batchelor

Oxford

Professor T.B. Benjamin

Cranfield Inst. of Technology

Professor J.L. Stollery

Imperial College

Professor P. Bradshaw

Professor J.T. Stuart

Universities and Colleges

ANU

Library

Professor J.S. Turner, Research School of Earth Sciences

Adelaide

Barr Smith Library

Professor R.E. Luxton, Dept of Mechanical Engineering

Flinders

Library

La Trobe

Library

Melbourne

Engineering Library

Professor P.N. Joubert, Department of Mechanical Engineering

Professor A.E. Perry, Department of Mechanical Engineering

Monash

Hargrave Library

Professor W.H. Melbourne, Department of Civil Engineering

Professor B.R. Morton, Department of Mathematics

Newcastle

Library

New England

Library

Sydney

Engineering Library

Professor G.A. Bird, Department of Aeronautical Engineering

NSW

Physical Sciences Library

Professor R.D. Archer, Department of Aeronautical Engineering

Professor P.T. Fink

Library, Australian Defence Force Academy

Queensland

Library

Professor R.J. Stalker, Department of Mechanical Engineering

Western Australia

Library

RMIT

Library

CANADA

NRC

National Aeronautical Establishment

Mr G.F. Marsters (Director)

DISTRIBUTION

AUSTRALIA

Department of Defence

Defence Central

Chief Defence Scientist
Assist Chief Defence Scientist, Operations (shared copy)
Assist Chief Defence Scientist, Policy (shared copy)
Director, Departmental Publications
Counsellor, Defence Science (London) (Doc Data Sheet Only)
Counsellor, Defence Science (Washington) (Doc Data Sheet Only)
S.A. to Thailand MRD (Doc Data Sheet Only)
S.A. to DRC (Kuala Lumpur) (Doc Data Sheet Only)
OIC TRS, Defence Central Library
Document Exchange Centre, DISB (18 copies)

Aeronautical Research Laboratory

Director
Library
Chief - Aerodynamics and Aero Propulsion Division
Head - Aerodynamics Branch
Divisional File - Aerodynamics and Aero Propulsion
Authors: G. L. Brown
J.M. Lopez

Defence Science & Technology Organisation - Salisbury Library

WSRL

Maritime Systems Division (Sydney)

Navy Office

Navy Scientific Adviser (3 copies Doc Data Sheet)
Director of Naval Aircraft Engineering (Doc Data Sheet Only)

Army Office

Scientific Adviser - Army (Doc Data sheet only)

Air Force Office

Air Force Scientific Adviser
Director General Aircraft Engineering - Air Force
(Doc Data sheet only)

Department of Administrative Services

Bureau of Meteorology, Library

Statutory and State Authorities and Industry

Aerospace Technologies Australia, Library
Hawker de Havilland Aust Pty Ltd, Bankstown, Library
CSIRO
Chief, Division of Oceanography
Chief, Division of Energy Technology
Chief, Division of Atmospheric Sciences

DOCUMENT CONTROL DATA

PAGE CLASSIFICATION
UNCLASSIFIED
PRIVACY MARKING

1a. AR NUMBER AR-004-573	1b. ESTABLISHMENT NUMBER ARL-AERO-R-174	2. DOCUMENT DATE JANUARY 1988	3. TASK NUMBER DST 85/025
4. TITLE AXISYMMETRIC VORTEX BREAKDOWN PART II: PHYSICAL MECHANISMS		5. SECURITY CLASSIFICATION (PLACE APPROPRIATE CLASSIFICATION IN BOX (S) IE. SECRET (S), CONFIDENTIAL (C), RESTRICTED (R), UNCLASSIFIED (U)) <div style="display: flex; justify-content: space-around;"> <div><input type="checkbox"/> U DOCUMENT</div> <div><input type="checkbox"/> U TITLE</div> <div><input type="checkbox"/> U ABSTRACT</div> </div>	6. No. PAGES 32 7. No. REFS. 14
8. AUTHOR(S) G.L. BROWN J.M. LOPEZ		9. DOWNGRADING/DELIMITING INSTRUCTIONS	
10. CORPORATE AUTHOR AND ADDRESS AERONAUTICAL RESEARCH LABORATORY P.O. BOX 4331, MELBOURNE VIC. 3001		11. OFFICE/POSITION RESPONSIBLE FOR SPONSOR <u> DSTO </u> SECURITY <u> </u> DOWNGRADING <u> </u> APPROVAL <u> </u>	
12. SECONDARY DISTRIBUTION (OF THIS DOCUMENT) Approved for public release.			
OVERSEAS ENQUIRIES OUTSIDE STATED LIMITATIONS SHOULD BE REFERRED THROUGH ASDIS, DEFENCE INFORMATION SERVICES BRANCH, DEPARTMENT OF DEFENCE, CAMPBELL PARK, CANBERRA, ACT 2601			
13a. THIS DOCUMENT MAY BE ANNOUNCED IN CATALOGUES AND AWARENESS SERVICES AVAILABLE TO..... No limitations			
13b. CITATION FOR OTHER PURPOSES (IE. CASUAL ANNOUNCEMENT) MAY BE <input checked="" type="checkbox"/> UNRESTRICTED OR <input type="checkbox"/> AS FOR 13a.			
14. DESCRIPTORS Equations of motion Vortex breakdown		15. DFOA SUBJECT CATEGORIES 0046B 0051A	
16. ABSTRACT In Part I of this study (Lopez, 1988), numerical solutions of the axisymmetric Navier-Stokes equations are presented and compared with results from experiments for a confined cylindrical flow. The details of the vortex breakdown phenomenon are calculated with a high degree of accuracy. From solutions over a range of parameters the essential features of the flow are obtained. These solutions also provide flow quantities such as the vorticity and the pressure throughout the volume which would be difficult to obtain from experiments. In this paper the solutions are explored and insight into the essential physical mechanisms of vortex breakdown in this particular geometry are identified. These mechanisms, which rely on the production of			

PAGE CLASSIFICATION

UNCLASSIFIED

PRIVACY MARKING

THIS PAGE IS TO BE USED TO RECORD INFORMATION WHICH IS REQUIRED BY THE ESTABLISHMENT FOR ITS OWN USE BUT WHICH WILL NOT BE ADDED TO THE DISTIS DATA UNLESS SPECIFICALLY REQUESTED.

16. ABSTRACT (CONT.)

a negative azimuthal component of vorticity as a result of the stretching and tilting of the predominantly axially directed vorticity vector, are elucidated with the aid of a simple, steady, inviscid, axisymmetric equation of motion. This equation has been a starting point for most studies of vortex breakdown but a departure in the present study is that it is explored directly and not through perturbations of an initial stream function. The findings are then generalised to the case of vortex breakdown in swirling pipe flows.

17. IMPRINT

AERONAUTICAL RESEARCH LABORATORY, MELBOURNE

18. DOCUMENT SERIES AND NUMBER

AERODYNAMICS REPORT 174

19. COST CODE

54 5006

20. TYPE OF REPORT AND PERIOD COVERED

21. COMPUTER PROGRAMS USED

22. ESTABLISHMENT FILE REF. (S)

23. ADDITIONAL INFORMATION (AS REQUIRED)

DOCUMENT CONTROL DATA

PAGE CLASSIFICATION
UNCLASSIFIED

PRIVACY MARKING

1a. AR NUMBER AR-004-573	1b. ESTABLISHMENT NUMBER ARL-AERO-R-174	2. DOCUMENT DATE JANUARY 1988	3. TASK NUMBER DST 85/025
4. TITLE AXISYMMETRIC VORTEX BREAKDOWN PART II: PHYSICAL MECHANISMS		5. SECURITY CLASSIFICATION (PLACE APPROPRIATE CLASSIFICATION IN BOX(S) IE. SECRET (S), CONF.(C) RESTRICTED (R), UNCLASSIFIED (U)). <div style="display: flex; justify-content: space-around;"> <div style="border: 1px solid black; padding: 2px; text-align: center;">U</div> <div style="border: 1px solid black; padding: 2px; text-align: center;">U</div> <div style="border: 1px solid black; padding: 2px; text-align: center;">U</div> </div> <div style="display: flex; justify-content: space-around; font-size: small;"> DOCUMENT TITLE ABSTRACT </div>	6. NO. PAGES 52
8. AUTHOR(S) G.L. BROWN J.M. LOPEZ		9. DOWNGRADING/DELIMITING INSTRUCTIONS	
10. CORPORATE AUTHOR AND ADDRESS AERONAUTICAL RESEARCH LABORATORY P.O. BOX 4331, MELBOURNE VIC 3001		11. OFFICE/POSITION RESPONSIBLE FOR: SPONSOR <u>DSTO</u> SECURITY <u>-</u> DOWNGRADING <u>-</u> APPROVAL <u>-</u>	
12. SECONDARY DISTRIBUTION (OF THIS DOCUMENT)		Approved for public release.	
OVERSEAS ENQUIRIES OUTSIDE STATED LIMITATIONS SHOULD BE REFERRED THROUGH ASDIS, DEFENCE INFORMATION SERVICES BRANCH, DEPARTMENT OF DEFENCE, CAMPBELL PARK, CANBERRA, ACT 2601			
13a. THIS DOCUMENT MAY BE ANNOUNCED IN CATALOGUES AND AWARENESS SERVICES AVAILABLE TO.... No limitations.			
13b. CITATION FOR OTHER PURPOSES (IE. CASUAL ANNOUNCEMENT) MAY BE		<input checked="checked" type="checkbox"/> UNRESTRICTED OR <input type="checkbox"/> AS FOR 13a.	
14. DESCRIPTORS Equations of motion Vortex breakdown		15. DRDA SUBJECT CATEGORIES 0046B 0051A	
16. ABSTRACT In Part I of this study (Lopez, 1988), numerical solutions of the axisymmetric Navier-Stokes equations are presented and compared with results from experiments for a confined cylindrical flow. The details of the vortex breakdown phenomenon are calculated with a high degree of accuracy. From solutions over a range of parameters the essential features of the flow are obtained. These solutions also provide flow quantities such as the vorticity and the pressure throughout the volume which would be difficult to obtain from,			

PAGE CLASSIFICATION
UNCLASSIFIED

PRIVACY MARKING

THIS PAGE IS TO BE USED TO RECORD INFORMATION WHICH IS REQUIRED BY THE ESTABLISHMENT FOR ITS OWN USE BUT WHICH WILL NOT BE ADDED TO THE DISTIS DATA UNLESS SPECIFICALLY REQUESTED.

16. ABSTRACT (CONT.)

experiments. In this paper the solutions are explored and the essential physical mechanisms of vortex breakdown in this particular geometry are identified. These mechanisms, which rely on the production of a negative azimuthal component of vorticity as a result of the stretching and tilting of the predominantly axially directed vorticity vector, are elucidated with the aid of a simple, steady, inviscid, axisymmetric equation of motion. This equation has been a starting point for most studies of vortex breakdown but a departure in the present study is that it is explored directly and not through perturbations of an initial stream function. The findings are then generalised to the case of vortex breakdown in swirling pipe flows. *Australian J. Sci. 1981*

17. IMPRINT

AERONAUTICAL RESEARCH LABORATORY, MELBOURNE

18. DOCUMENT SERIES AND NUMBER

AERODYNAMICS REPORT 174

19. COST CODE

54 5006

20. TYPE OF REPORT AND PERIOD
COVERED

21. COMPUTER PROGRAMS USED

22. ESTABLISHMENT FILE REF.(S)

23. ADDITIONAL INFORMATION (AS REQUIRED)